

TALLINN UNIVERSITY OF TECHNOLOGY  
School of Information Technologies

Rudolf Põldma 212087IVEM

# **Development of a Prototype Piezoelectric Pump Driver for a Lab-on-Chip Device**

Master's thesis

Supervisor: Rauno Jõemaa

MSc

Co Supervisor: Tamás Pardy

PhD

Tallinn 2023

TALLINNA TEHNIKAÜLIKOOL  
Infotehnoloogia teaduskond

Rudolf Põldma 212087IVEM

# **Piesoelektrilise pumba juhtseadme prototüübi arendus labor kiibil seadmele**

Magistritöö

Juhendaja: Rauno Jõemaa

MSc

Kaasjuhendaja: Tamás Pardy

PhD

Tallinn 2023

## **Author's declaration of originality**

I hereby certify that I am the sole author of this thesis. All the used materials, references to the literature and the work of others have been referred to. This thesis has not been presented for examination anywhere else.

Author: Rudolf Põldma

07.05.2023

## **Abstract**

Piezoelectric micropumps have emerged as a promising solution for precise fluid control in lab-on-chip devices. However, developing a reliable and efficient piezoelectric micropump driver that can be integrated with a lab-on-chip system remains a challenge.

This study presents the development of a prototype piezoelectric pump driver for a lab-on-chip device. The driver was designed to be able to generate wide variety of frequencies, amplitudes and waveforms with the purpose of being able to create microfluidic droplets.

The design of the driver used a combination of commercially available components. It consisted of several key circuit blocks, including signal generation, signal first stage amplification, amplitude control, and second stage amplification powered by a boost converter.

The driver underwent testing to assess its pressure capabilities across various frequencies, amplitudes, and waveforms. The results indicated that the prototype driver could achieve a maximum average pressure of 58 kPa at 190 Hz. These findings confirmed the driver's ability to generate the necessary pressure for droplet generation.

However, further development is required to enhance its versatility and size for broader applications.

The proposed piezoelectric pump driver has the potential to be used in a variety of lab-on-chip devices, enabling rapid and efficient analysis of biological samples with great accuracy and sensitivity.

This thesis is written in English and is 42 pages long, including 6 chapters, 41 figures and 10 tables.

## Annotatsioon

Piesoelektrilised mikropumbad on paljulubavaks lahenduseks vedeliku täpseks juhtimiseks labor-kiibil seadmetel. Siiski on väljakutseks usaldusväärse ja tõhusa piesoelektrilise mikropumba juhtseadme väljatöötamine, mida saaks integreerida labor-kiibil seadmega.

Magistritöös antakse ülevaade piesoelektrilise pumba juhtseadme prototüübi väljatöötamisest labor-kiibil seadme jaoks. Loodud juhtseade suudab genereerida erinevaid sagedusi, amplituude ja lainekujusid eesmärgiga luua mikrofluidipiiskusid.

Piesoelektrilise pumba juhtseadmes kasutati kõigile kättesaadavaid komponente. Juhtseade koosnes mitmest plokist - signaali genereerimine, signaali esimese astme võimendus, amplituudi reguleerimine ja teise astme võimendus, mille toiteallikaks on võimendusmuundur.

Juhtseadme võimet tekitada rõhku testiti erinevatel sagedustel, amplituudidel ja lainekujudel. Tulemused näitasid, et juhtseade on võimeline saavutama maksimaalse keskmise rõhu 58 kPa sagedusel 190 Hz. Mõõtmised kinnitasid, et juhtseade suudab tekitada piiskade genereerimiseks vajalikku rõhku. Siiski on vaja juhtseadet edasi arendada, et vähendada seadme suurust ja võimaldada selle laiemat kasutust.

Piesoelektrilise pumba juhtseadet saab kasutada mitmesugustes labori-kiibil asuvates seadmetes, võimaldades bioloogiliste proovide kiiret ja tõhusat analüüsi suure täpsuse ja tundlikkusega.

Lõputöö on kirjutatud inglise keeles ning sisaldab teksti 42 leheküljel, 6 peatükki, 41 joonist, 10 tabelit.

## List of abbreviations and terms

DAC	Digital-to-Analog Converter
DNA	Deoxyribonucleic Acid
ETAG	Estonian Research Council
GUI	Graphical User Interface
IVD	In Vitro Diagnostics
LoC	Lab-on-a-Chip
MCU	Microcontroller Unit
MEMS	Microelectromechanical Systems
MOSFET	Metal-Oxide-Semiconductor Field-Effect Transistor
NMOS	N-channel Metal-Oxide-Semiconductor
OPAMP	Operational Amplifier
PCB	Printed Circuit Board
PWM	Pulse Width Modulation
SPI	Serial Peripheral Interface

## Table of contents

1 Introduction .....	12
1.1 Design requirements .....	13
1.2 Objectives .....	13
2 State of the art.....	15
2.1 Lab-on-a-Chip, microfluidics and droplet microfluidics.....	15
2.1.1 Lab-on-a-Chip .....	15
2.1.2 Microfluidics .....	16
2.1.3 Droplet microfluidics.....	17
2.2 Piezoelectric pump .....	19
2.3 Piezoelectric pump driving circuit components .....	20
2.3.1 Microcontroller.....	20
2.3.2 Driver circuit .....	20
2.3.3 Boost converter.....	21
2.3.4 Signal generation methods .....	22
2.3.5 Signal amplification methods .....	23
2.3.6 Existing piezoelectric drivers .....	26
3 Development.....	32
3.1 Planning .....	32
3.2 Analysis and models.....	32
3.3 Prototype board.....	34
3.4 Designing the PCB .....	36
4 Experimental analysis.....	37
4.1 Frequency measurements with distilled water.....	38
4.2 Amplitude measurements with distilled water .....	40
4.3 Waveform measurements with distilled water .....	41
4.4 Frequency measurements with oil .....	44
4.5 Amplitude measurements with oil.....	45
4.6 Droplet generation simulations.....	47
4.7 Comparison to existing driver .....	50

5 Future developments .....	52
5.1 Next iteration PCB.....	52
5.2 Create library/GUI for driver.....	52
5.3 Add output voltage and boost converter feedback .....	52
6 Summary.....	54
References .....	55
Appendix 1 – Non-exclusive licence for reproduction and publication of a graduation thesis .....	59



## List of figures

Figure 1. Development flowchart.....	14
Figure 2. Lab-on-a-chip device [10].....	16
Figure 3. Size characteristics of microfluidic devices [16]. ....	17
Figure 4. Droplet generation [18]. ....	17
Figure 5. Flow-focusing junction configuration [20]. ....	18
Figure 6. T-junction configuration [21].....	18
Figure 7. Bartels Mikrotechnik functional principle of the piezoelectric micropump [23]. .....	19
Figure 8. Exploded view of Bartels Mikrotechnik micropump [24]. ....	19
Figure 9. Bartels Mikrotechnik mp-Highdriver pumping water [29]. ....	21
Figure 10. A basic boost converter circuit.....	21
Figure 11. Wien bridge oscillator circuit.....	22
Figure 12. Basic R-2R ladder. ....	23
Figure 13. Incorrectly set Q-point [38].....	24
Figure 14. Inverting and noninverting operational amplifiers.....	25
Figure 15. Inverting operational amplifier with noninverting positive reference voltage. .....	26
Figure 16. Bartels Mikrotechnik mp-Highdriver [41]. ....	26
Figure 17. PiezoDrive PDu100b driver [42]. ....	27
Figure 18. Microchip piezoelectric micropump demo board [43].....	28
Figure 19. Microchip high voltage driver board block diagram [43].....	29
Figure 20. Piezoelectric droplet-on-demand generator [44].....	29
Figure 21. Input waveforms and the waveform appearing on the load. ....	30
Figure 22. Initial design flow chart. ....	32
Figure 23. Prototype circuit in LTspice.....	33
Figure 24. The waveforms of the signals supplied to the micropump. ....	34
Figure 25. Prototype board. ....	35
Figure 26. The output of the prototype while the micropump was connected and pumping.....	35

Figure 27. Final design in LTspice.....	36
Figure 28. 3D model of the final PCB design. ....	36
Figure 29. Driving signal labelling.....	37
Figure 30. Peak-to-peak amplitude values at maximum output and at 200 Hz.....	38
Figure 31. Average pressures with varying frequencies.....	39
Figure 32. Three highest average pressure frequencies.....	39
Figure 33. Average pressure during varying voltage measurements.....	40
Figure 34. Pressure during varying waveform measurements. ....	42
Figure 35. Instruction for appropriate handling [49].....	43
Figure 36. Peak-to-peak triangle wave amplitude values at 190 Hz. ....	44
Figure 37. Average pressure during varying frequency measurements with oil. ....	45
Figure 38. Three highest average pressure frequency (oil). ....	45
Figure 39. Average pressure with varying amplitude (oil).....	46
Figure 40. Bartels mikrotechnik mp-Highdriver pressure measurements [29]. ....	50
Figure 41. Average pressure measurements for driver comparison. ....	51

## List of tables

Table 1. Design requirements.....	13
Table 2. Comparison between existing drivers. ....	30
Table 3. Digital potentiometer values for varying frequency.....	39
Table 4. Digital potentiometer values during varying voltage measurements. ....	40
Table 5. Peak-to-peak values during varying amplitude measurements. ....	41
Table 6. Digital potentiometer values during varying waveform measurements.....	42
Table 7. Voltage values during varying waveform measurements. ....	42
Table 8. Digital potentiometer values during varying amplitude measurements (oil)...	46
Table 9. Voltage values during varying amplitude measurements (oil).....	46
Table 10. Droplet generation simulation results from COMSOL .....	47

## 1 Introduction

Microfluidics involves manipulating fluids in channels that have dimensions in the range of tens of micrometres. The technology provides a wide range of applications in fields such as medicine, chemistry, biology, and physical sciences. The ability to work with very small volumes of samples and reagents allows for high resolution and sensitivity in analyses. Microfluidics has found applications in various fields, including medicine, chemistry, biology, and physical sciences. In medicine, microfluidic devices are used for point-of-care diagnostics, drug discovery, and personalized medicine [1], [2]. Droplet-based microfluidics is one of the branches of microfluidics, it focuses on creating discrete fluid packets in the form of microdroplets to handle fluids in a precise and reliable manner [3]–[5]. This method allows to reduce the volume of reagent used in assays, reduces sample and equipment sizes while enhancing the speed of biological and chemical assays [3]. Droplet generation in microfluidics is characterized by three main factors: droplet size, generation rate, and coefficient of variation. Various applications require specific combinations of these three characteristics, which influences the selection of pumping mechanisms. Different pumping mechanisms vary in their minimum required infrastructure, producible flow rate range, and flow rate stability. [6], [7]

In the TalTech project PRG620, a portable microfluidic pumping device was developed for droplet generation. The project opted for a piezoelectric pumping mechanism due to its advantages, such as low cost, small profile, and flow regulation at low flow rates, which suited the project's needs. The piezoelectric pumping solution consists of a piezo element and a piezo driver. However, as this pumping solution is uncommon in microfluidics and droplet microfluidics, the market for piezo pump drivers is limited. The few available solutions are expensive and lack portable, target-oriented designs.

The objective of this work is to develop a customized piezoelectric pump driver for the droplet generation device that was created in PRG620. The driver should allow for adjustable frequency, amplitude, and waveform, and should be controlled via SPI communication. The design should use components with currently available technology

while balancing cost and quality. All components should be off-the-shelf and widely accessible. The design should incorporate a boost converter to raise the battery voltage to the necessary level for the piezoelectric pump. The driver's properties are assessed and compared to those of existing off-the-shelf drivers.

## 1.1 Design requirements

The requirements for the driver are shown on Table 1.

Table 1. Design requirements.

Property	Min	Max
Output voltage	50 V	200V
Frequency	50 Hz	10 kHz
Amplitude	1 V	-
Digitally controlled	-	-
Plug and Play (no external components)	-	-

## 1.2 Objectives

The objective of this work is to design a specialized piezoelectric pump driver for the droplet generation device.

- Design and develop a PCB to demonstrate applicability to existing microfluidic infrastructure (related to ETAG project PRG620)
- Benchmark the driver against competitive drivers.

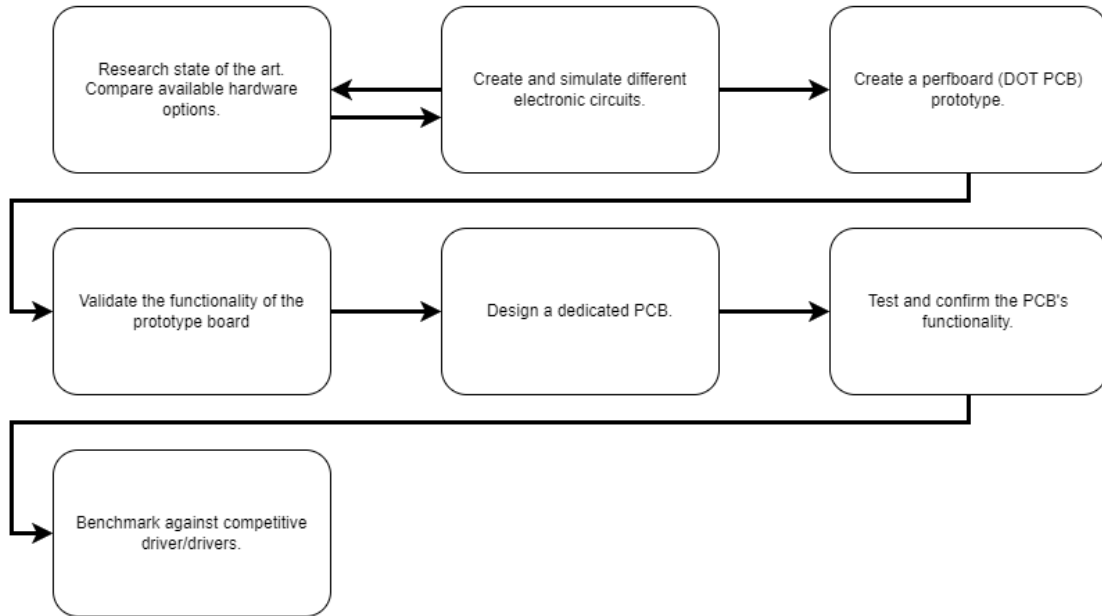


Figure 1. Development flowchart.

## **2 State of the art**

This chapter provides an introduction to Lab-on-a-Chip and microfluidics, including piezoelectric pumps, followed by a review of hardware components in a piezoelectric pump driver. Finally, the chapter includes an overview of existing commercial piezoelectric pump drivers available in the market.

### **2.1 Lab-on-a-Chip, microfluidics and droplet microfluidics**

#### **2.1.1 Lab-on-a-Chip**

The focus of Lab-on-a-Chip (LoC) technology is to integrate laboratory functions into a single fluidic circuit that occupies only a few square millimetres or centimetres. The technology uses microfluidics for the handling of fluids automatically, using small volumes of liquid down to nanolitres or even picolitres. Compared to traditional laboratory instrumentation, LoC offers several advantages, including lower fluid volumes and reagent costs, faster analyses, compactness, and lower fabrication costs. In vitro diagnostics (IVD), the technology has enabled the development of complex rapid diagnostic tests that can be performed at home and whose performance is comparable to clinical diagnostics. LoC devices are typically considered a subset of micro-electro-mechanical systems (MEMS) and often rely on integrated microelectronic sensors and actuators due to their high level of integration. [8], [9]

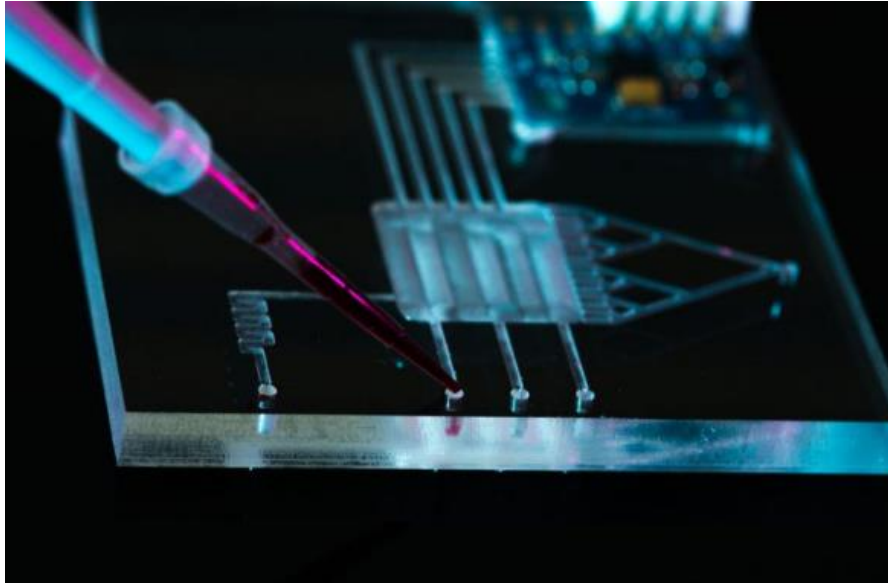


Figure 2. Lab-on-a-chip device [10].

Currently, most LoC technologies are not yet suitable for industrialization. Even in their core application of ultra-multiplex diagnosis, the standard fabrication technologies are still uncertain. Also, LoC devices require external systems to function properly. Despite their small size and power, these devices need specific machinery such as electronics or flow control systems to accurately inject, split, and position samples. The use of external equipment can increase the overall system size and cost, and some components, particularly flow control systems, may pose limitations on the performance of lab-on-a-chip devices. [9]

### **2.1.2 Microfluidics**

Microfluidics involves manipulating fluids in channels that have dimensions in the range of tens of micrometres. The technology provides a wide range of applications in fields such as medicine, chemistry, biology, and physical sciences. The ability to work with very small volumes of samples and reagents allows for high resolution and sensitivity in analyses. Fluid behaviour is significantly different in microscale, as compared to macroscale. For example, when the mass of the fluid reduces, the impact of viscosity becomes more dominant than inertia. Reducing the channel size results in a higher surface-to-volume ratio, which amplifies the significance of surface-related effects such as adsorption, capillary action, surface wetting. [11]–[13].

Microfluidics has found applications in various fields, including medicine, chemistry, biology, and physical sciences. In medicine, microfluidic devices are used for point-of-



care diagnostics, drug discovery, and personalized medicine [1], [2]. In chemistry, microfluidics is used for chemical synthesis, reaction optimization, and high-throughput screening [14]. In biology, microfluidics is used for cell culture, DNA analysis, and protein analysis [15].

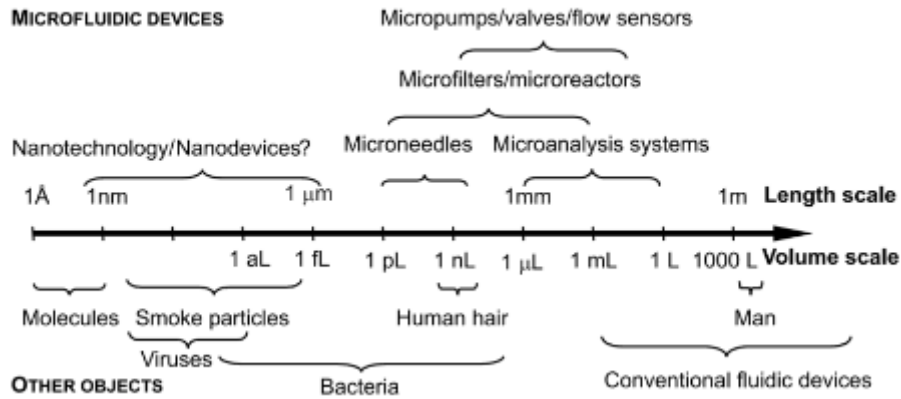


Figure 3. Size characteristics of microfluidic devices [16].

### 2.1.3 Droplet microfluidics

In microfluidics, a droplet is defined as a spherical or nearly spherical volume of liquid or gel that is suspended in an immiscible fluid, which refers to liquids that do not mix to form a homogeneous solution. [3], [17].

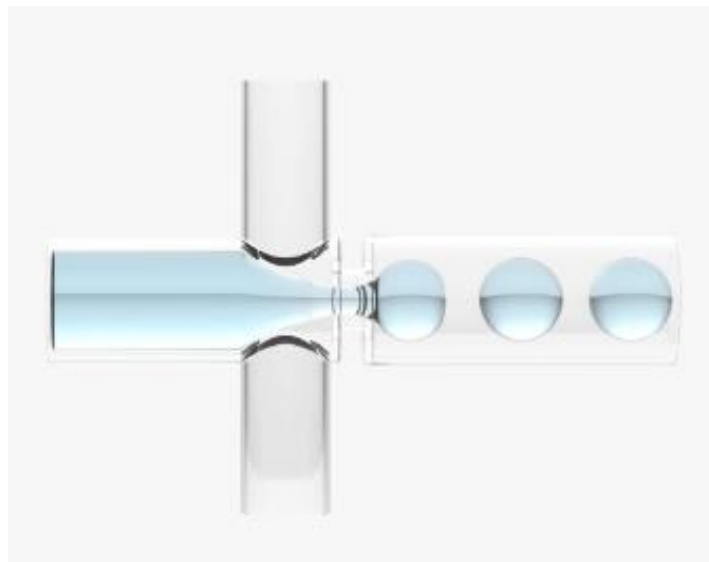


Figure 4. Droplet generation [18].

Droplet-based microfluidics is one of the branches of microfluidics, it focuses on creating discrete fluid packets in the form of microdroplets to handle fluids in a precise and reliable

manner [3]–[5]. This method allows to reduce the volume of reagent used in assays, reduces sample and equipment sizes while enhancing the speed of biological and chemical assays [3].

Two primary methods used for generating droplets and particles using microfluidics are flow-focusing junction and T-junction [3]. In a flow-focusing configuration, a narrow region in a microfluidic device is used to force the dispersed and continuous phase through it, this results in the generation of droplets [4], [19].

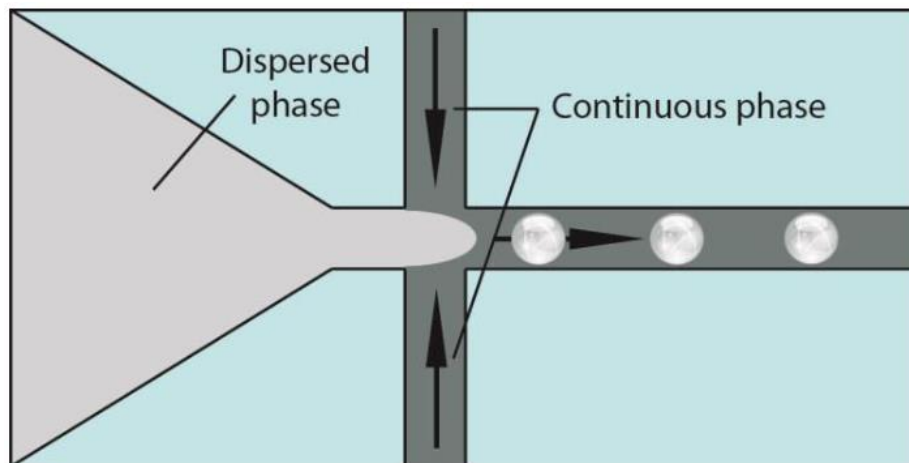


Figure 5. Flow-focusing junction configuration [20].

Droplets are generated in a T-junction configuration when the continuous phase flows through the dispersed phase channel perpendicularly [21].

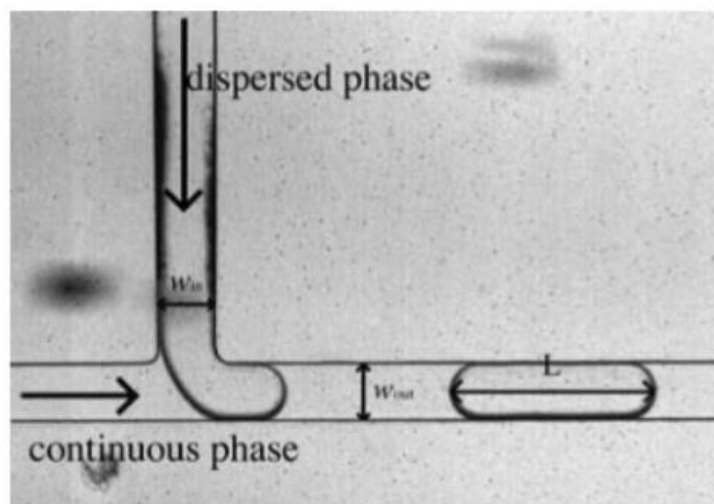


Figure 6. T-junction configuration [21].

## 2.2 Piezoelectric pump

Piezoelectricity is generated when mechanical stress is subjected to a piezoelectric material. The mechanical stress generates an electric charge in the material that is directly proportional to the force applied. This effect is reversible, so by applying electrical energy to a piezoelectric material it will strain. [22]

A piezoelectric pump uses this effect to pump liquids or gases, by deforming and forming of the pump membrane. As upwards stroke pulls the liquids to the chamber, the downward stroke pushes the liquid from the chamber. Check valves are used to define the flow direction. The working principle is visualized in Figure 7 [23].

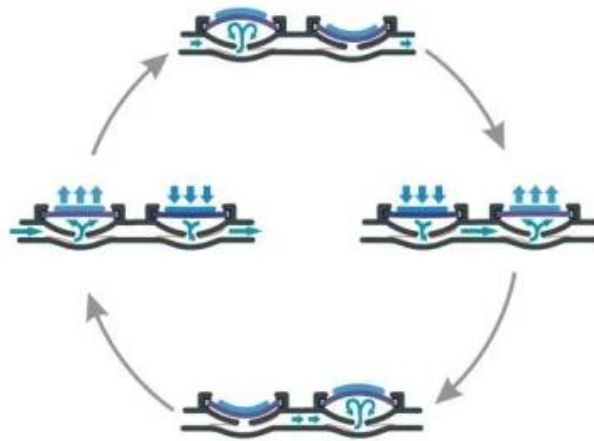


Figure 7. Bartels Mikrotechnik functional principle of the piezoelectric micropump [23].

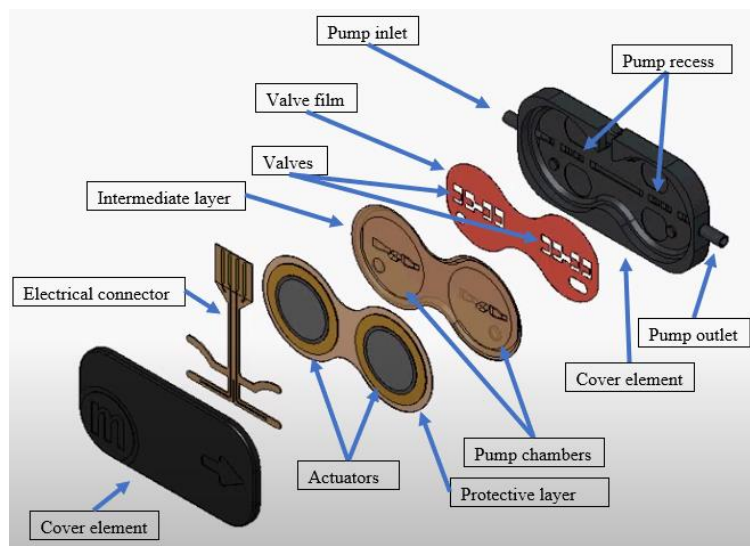


Figure 8. Exploded view of Bartels Mikrotechnik micropump [24].

As the piezoelectric actuators deform in response to the applied voltage, they create pressure fluctuations within the pump chamber (Figure 8). This deformation causes the

check valves to open and close alternatively. This allows fluid to be drawn into the pump chamber during the expansion phase and expelled during the contraction phase. [25]

In order to generate the required driving signals for a piezoelectric crystal, a driver is needed. The components and logic behind the driver are discussed in the next section along with existing solutions.

## **2.3 Piezoelectric pump driving circuit components**

### **2.3.1 Microcontroller**

A microcontroller is a compact and specialized single-chip computer designed to perform specific tasks within a device [26]. With numerous microcontrollers available in the market for different features and intended uses, the key differences between them include CPU speed, memory size, peripheral variety, and cost. When selecting a microcontroller, it is essential to consider the number of digital or analogue inputs and outputs the controller needs to control, its processing speed, and the type of communication it uses.

### **2.3.2 Driver circuit**

A driver is the interface between an actuator and a microcontroller. A driver can control the speed, torque, and direction of the motor or an actuator. [27]

The voltage required to drive a piezoelectric pump depends on the size of the piezoelectric element and range of motion. The voltage required to create the electric field is relatively high. [28] For a piezoelectric driver powered by batteries, it is crucial to be able to boost the battery voltage to meet the necessary level.

To control the flowrate of a liquid or gas, the driver must be able to vary the frequency and voltage of the output waveform (Figure 9).

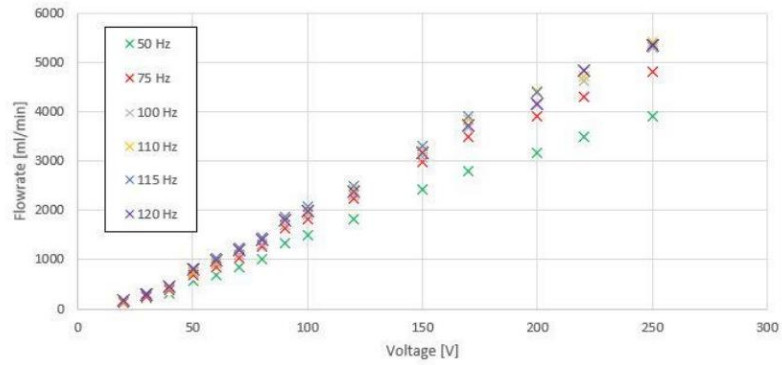


Figure 9. Bartels Mikrotechnik mp-Highdriver pumping water [29].

The ability to control a motor using various waveforms such as sine, triangular, and square waves is a valuable feature for a driver. Hence, a portable piezoelectric pump driver should be capable of producing different waveforms and frequencies while also boosting them to the necessary voltage level.

### 2.3.3 Boost converter

A boost converter is a DC-DC converter that is used to increase the input voltage. A basic boost converter is composed of an inductor, diode, a switching device and a capacitor (Figure 10). [30]

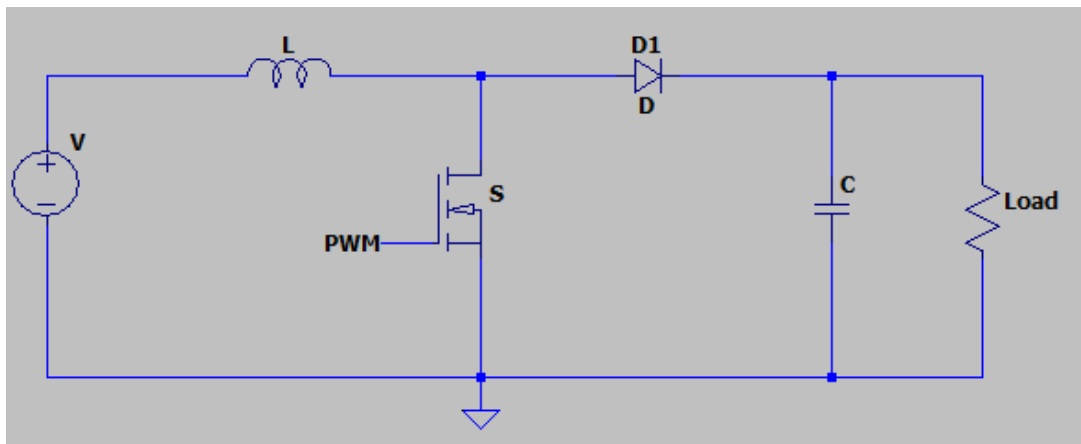


Figure 10. A basic boost converter circuit.

The switching device, in this case a NMOS, is controlled by a PWM signal. When the switch  $S$  is closed, the current flows through the inductor to the NMOS and back to the input voltage ground. During this time the diode  $D$  is in the reverse biased condition, so no current flows through it. Energy is stored in the magnetic field of inductor  $L$ , which is then transferred to the load when switch  $S$  is turned on. The current now flows through the inductor, capacitor, load and the diode. [30]

### 2.3.4 Signal generation methods

Signal generation is the process of creating an electrical signal with specific parameters, frequency, amplitude and waveform. The purpose of an electronic circuit is to transmit information in form of an electrical signal, there are many ways to generate signals. [31] In this chapter an analogue method of generating signals called a Wien bridge oscillator is described and a digital method called digital-to-analogue converter.

#### 2.3.4.1 Wien bridge oscillator

A Wien bridge oscillator uses a series and parallel RC circuit connected to a voltage divider to generate sinewaves. The values of the RC circuit determine the frequency of the oscillations. [32] When using equal sets of values for both RC circuits, the frequency can be calculated by equation 1 [32]:

$$f = \frac{1}{2\pi RC} \quad (1)$$

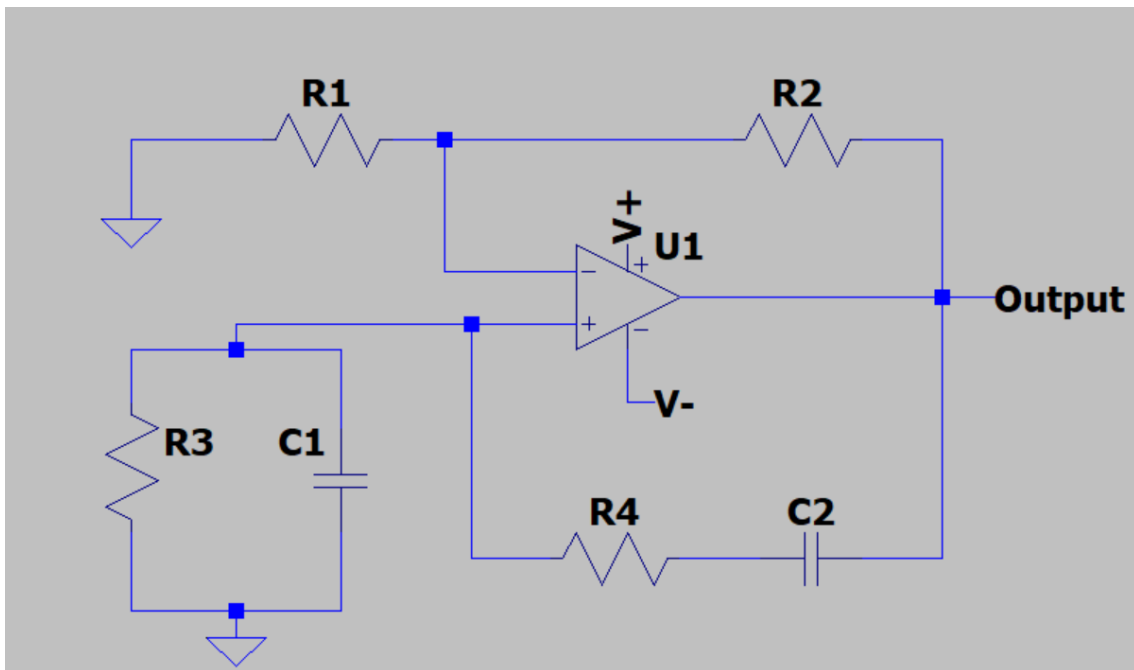


Figure 11. Wien bridge oscillator circuit.

In this circuit, R3 and C1 act as a low pass filter and R4, C2 as high pass filter (Figure 11). At low frequency the capacitor C2 acts like an open circuit, at high frequencies the capacitor C1 acts like an open circuit, so there is no output signal. [32]

### 2.3.4.2 Digital-to-analogue converter

A digital-to-analogue converter (DAC) is used to produce an analogue output from a digital input. One of the basic methods of how a DAC does this is the use of an R-2R ladder, on Figure 12 a 4-bit R-2R ladder is shown. [33]

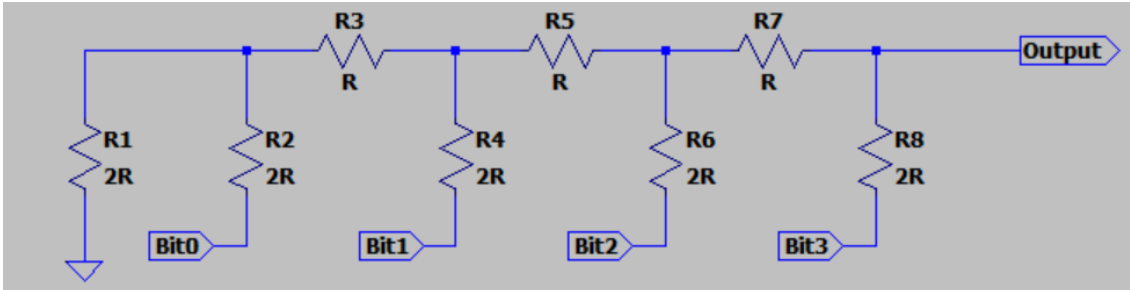


Figure 12. Basic R-2R ladder.

This design needs multiple resistors with 2 different values, value R and value 2R. A 4-bit R-2R ladder has 16 ( $2^{bits}$ ) possible outputs. The output voltage can be calculated by using the equation 2 [34]:

$$V_{out} = D \cdot \left( \frac{V_{ref}}{2^n} \right) \quad (2)$$

Where D is the binary value input (Bit 0 – Bit 3),  $V_{ref}$  is the input logic voltage level and  $n$  is the number of bits [34].

The advantage of the DAC is the possibility to control the output voltage digitally and generate different waveforms and frequencies.

### 2.3.5 Signal amplification methods

Increasing the amplitude of an input signal without distorting it in the process is called amplification. Devices that can do this are called amplifiers. Amplifier that amplifies the signal voltage is called a voltage amplifier, there are also current and power amplifiers. Amplifiers can be classified by the signal it is intended to amplify. Some amplifiers are intended to amplify audio frequency signals ranging 20 Hz to 20 kHz. Radio frequency amplifiers can amplify signals from 10 kHz up to 100 GHz. [35], [36]

#### 2.3.5.1 MOSFET amplifier

A circuit that contains a single metal-oxide-semiconductor field-effect transistor (MOSFET) can amplify the signal in three basic configurations, common-source,

common-drain and common-gate. For all configurations a quiescent point (Q-point) must be set, this is an operating point of the circuit when there is no input signal. When the Q-point is incorrectly set, it can lead to distortion, clipping and other non-linear effects (Figure 13). [37]

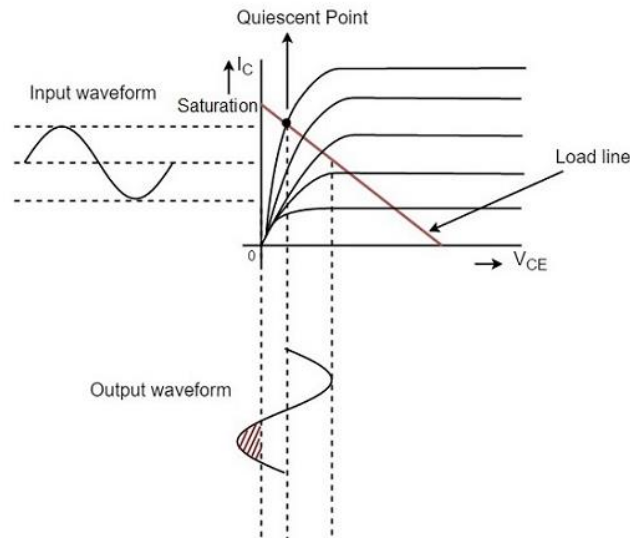


Figure 13. Incorrectly set Q-point [38].

The MOSFET amplifier is widely used and at least one of the three configurations mentioned before can be found in almost every amplifier's amplification stage. [37]

### 2.3.5.2 Operational amplifier

A typical operational amplifier (op amp) has two signal inputs, two power supply inputs and one output. The two signal inputs are called inverting (denoted with a "-") and noninverting (denoted with a "+") inputs. [39]



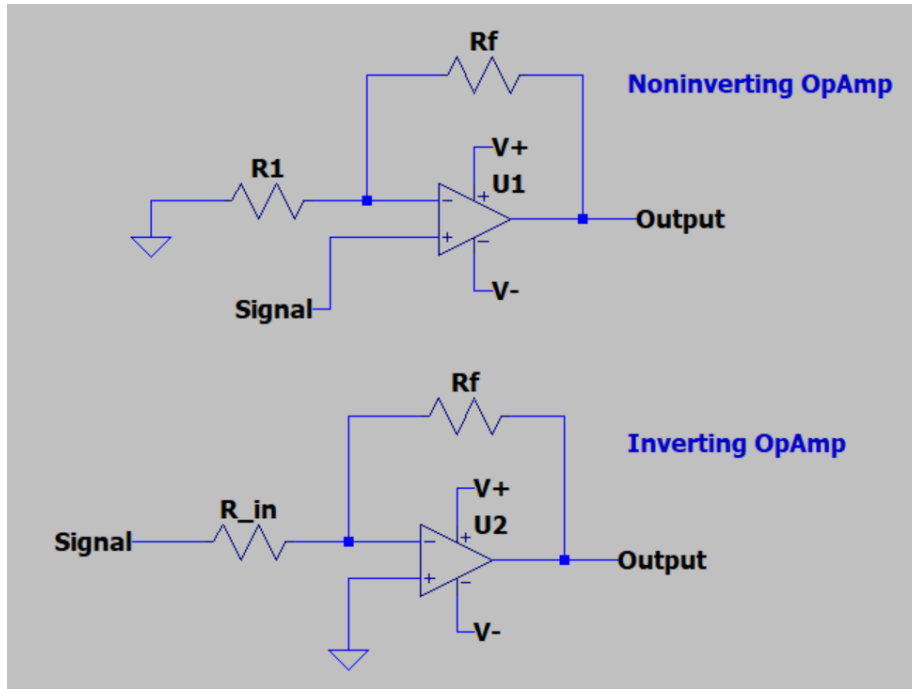


Figure 14. Inverting and noninverting operational amplifiers.

With two resistors, two basic operational amplifier circuits can be constructed, an inverting and noninverting (Figure 14). When using a noninverting op amp, the output signal is in phase with the output phase. [39]

The gain ( $A$ ) of a noninverting op amp can be calculated by equation 3.

$$A = 1 + \frac{R_f}{R_1} \quad (3)$$

An inverting op amp changes the polarity of the input signal and produces a  $180^\circ$  phase shift [39]. The gain is calculated by equation 4.

$$A = -\frac{R_f}{R_{in}} \quad (4)$$

When it is only necessary to phase shift the signal  $180^\circ$ , but not change the polarity of the signal, a noninverting positive voltage reference circuit should be added to the inverting op amp. The circuit is the same as inverting op amp, but with a voltage reference at the noninverting input (Figure 15). [40]

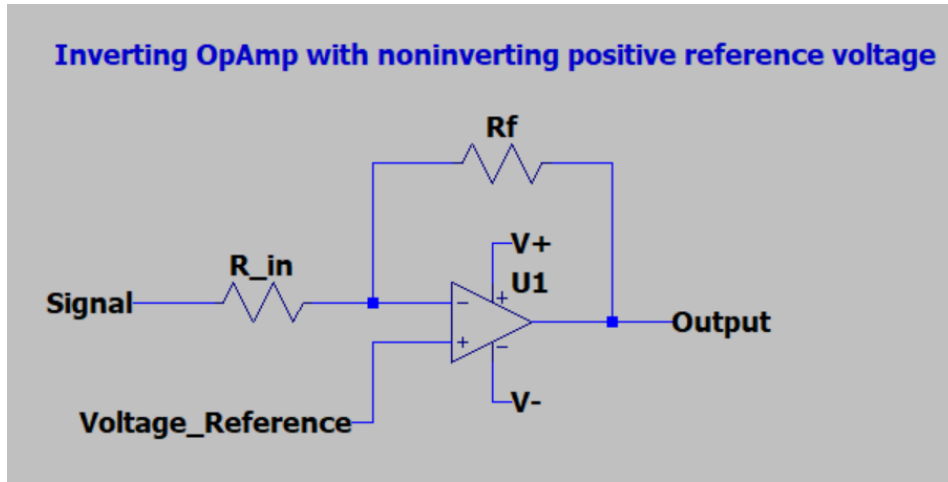


Figure 15. Inverting operational amplifier with noninverting positive reference voltage.

The equation to calculate the voltage reference is [40]:

$$V_{ref} = \frac{V_{out\_min} + V_{in\_max} \cdot \frac{R_f}{R_{in}}}{1 + \frac{R_f}{R_{in}}} \quad (5)$$

### 2.3.6 Existing piezoelectric drivers

The Bartels Mikrotechnik mp-Highdriver model has an input range of 2.7 V to 5.5 V and can produce a peak-to-peak output voltage of up to 250 V. The driver uses an I2C interface to control the waveform shape, peak-to-peak voltage, and boost-converter frequency. It provides a 5-bit resolution for setting the desired peak-to-peak voltage and a 3-bit resolution for the slew rate. To step up the input voltage, a boost converter with variable switching frequency is used. This is followed by a full-bridge output stage that converts the high voltage to an AC waveform suitable for driving the piezoelectric membrane pump. [41]



Figure 16. Bartels Mikrotechnik mp-Highdriver [41].

PiezoDrive PDU100b is a small linear amplifier used for driving piezoelectric actuators. It is possible to vary the gain and offset, change voltage ranges, and choose between

unipolar and bipolar inputs and outputs. It can drive two-wire piezoelectric actuators up to  $\pm 100$  V and three-wire up to +100 V. [42]



Figure 17. PiezoDrive PDU100b driver [42].

An external signal generator is needed to use this driver. The driver works by using a boost converter to generate a high-voltage from the supply voltage (3 – 5.5 V). The high voltage rail is used to supply the pair of complementary amplifiers. The signal from the external signal generator is used as input to the amplifiers and amplified to a higher voltage. The amplifier has a gain of 27.5, that means with a  $3.6 V_{p-p}$  input to the amplifiers, the output will be  $100 V_{p-p}$ . [7]

Microchip has created an application node demo to show how to drive a piezoelectric micropump using a Bartels mp6 Piezoelectric micropump. The demo system consists of a control board, high voltage driver board and an micropump. The high voltage driver board generates boosted signals with an adjustable frequency and peak-to-peak voltage to supply the micropump. [43]

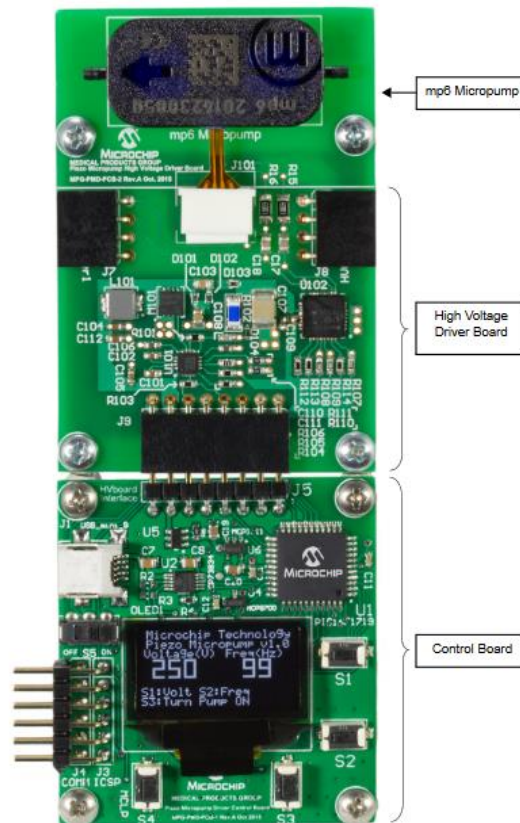


Figure 18. Microchip piezoelectric micropump demo board [43].

The driver operates by using a HV9150 boost converter to increase the input voltage to 250 V. The boosted voltage is supplied to HV513 serial-to-parallel converter that can be controlled by three primary inputs: Data in, Clock, and Latch enable pins. Two outputs are used to alternate the output between 200 V and -50 V, a clamping circuit is implemented to achieve the negative voltage. The waveform frequency can be adjusted by altering the clock speed, while the voltage level can be adjusted by the voltage reference pin on the boost converter (Figure 19). [43]

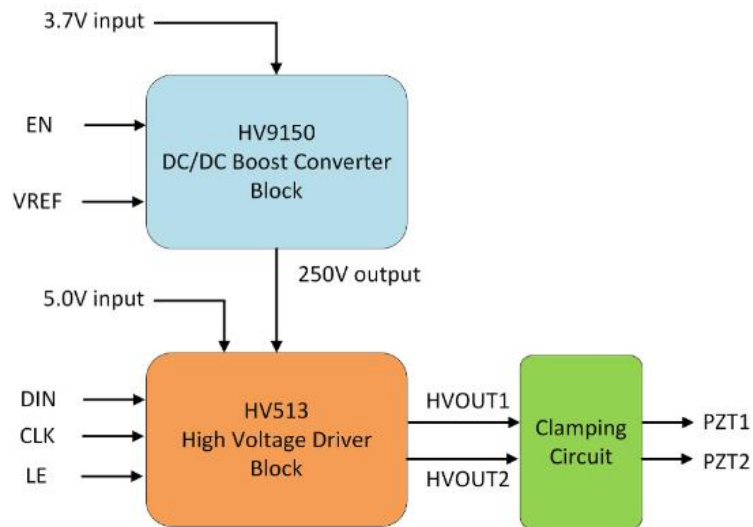


Figure 19. Microchip high voltage driver board block diagram [43].

A study introduced a piezoelectric droplet-on-demand generator that used a piezoelectric buzzer for droplet generation (Figure 20). The device used a peristaltic pump for liquid transportation, and just before the nozzle, a piezoelectric buzzer was employed to generate droplets. The droplet generator demonstrated the capability to produce droplets ranging from 0.5 to 1.4 mm in diameter. To drive the buzzer, the device used an Arduino Uno, a DC power supply with a voltage range of 0-72 V, and an H-bridge circuit. The H-bridge was connected to two output pins of the Arduino, enabling the driving of the buzzer and the reversal of polarity. To simplify the circuit, the device was designed to generate only square wave driving signals. [44]

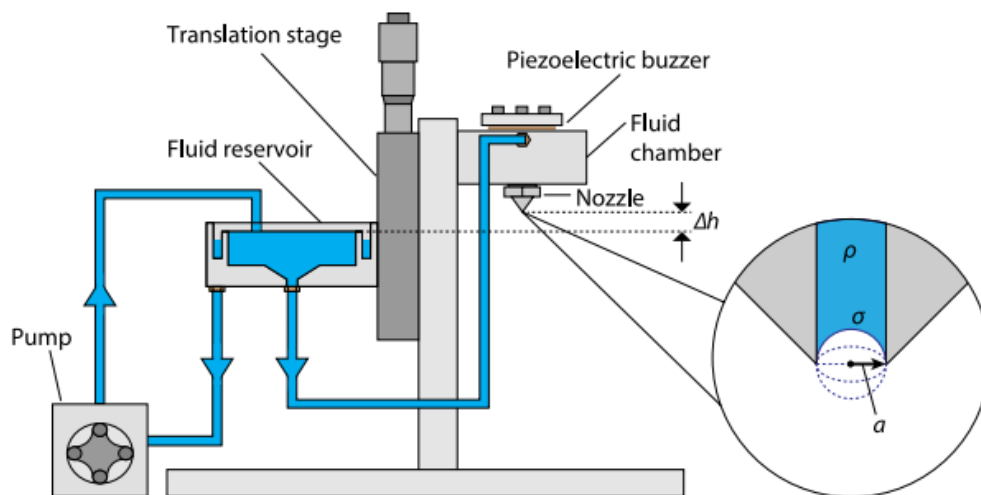


Figure 20. Piezoelectric droplet-on-demand generator [44].

According to an Apex Microtechnology publication [45], a piezoelectric actuator can be driven using a floating load configuration. This load type is not directly connected to the

power source or ground, and it offers the advantage of not requiring a negative supply voltage. By supplying two signals with a 180° phase shift to the load, the voltage swing is equal to the difference between the signal values. For example, if two 10 V sine waves with a 180° phase shift are supplied, the voltage on the load oscillates between 10 V and -10 V, as demonstrated in Figure 21.

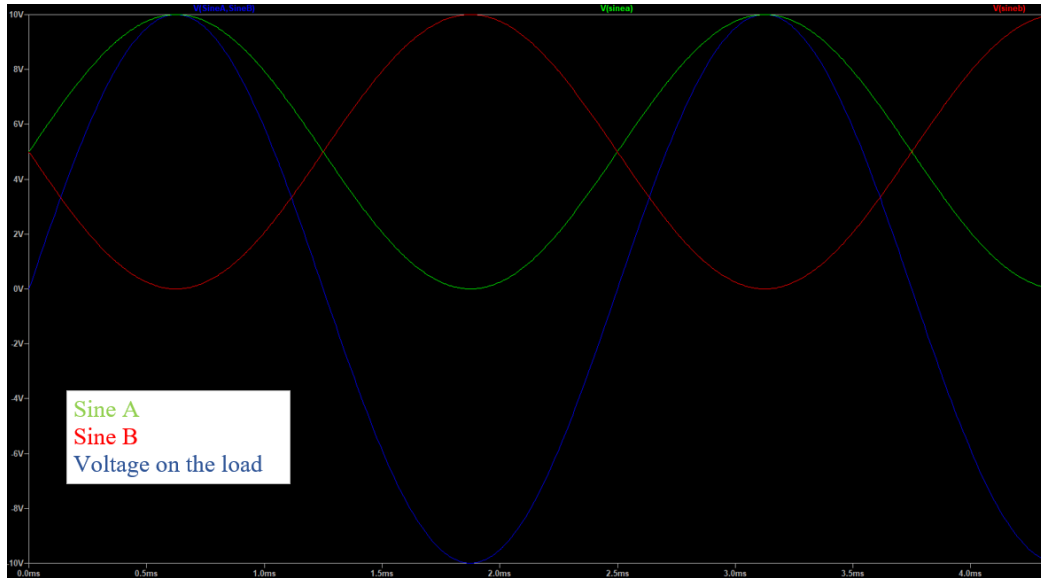


Figure 21. Input waveforms and the waveform appearing on the load.

Table 2 provides a comparison of the drivers, highlighting their main characteristics and features.

Table 2. Comparison between existing drivers.

Device	Bartels Mikrotechnik mp-Highdriver [41]	PiezoDrive PDu100b [46]	Microchip demo board [43]	Droplet-on-demand generator [44]
Amplitude range (V)	10 - 250	0 - 100	50 - 250	0 - 72
Frequency range (Hz)	50 - 800	5300 (at 100 V)	300 (at 250 V)	Not specified
Size (mm)	10.16 x 25.4	39 x 25	Not specified	Not specified
Pros	Plug and play	Easy to use	Design and component list	Easy circuit to replicate

			publicly available.	
Cons	Can't generate signals under 50 Hz	Requires an external signal generator	Can generate only one waveform	Needs an external power supply

## 3 Development

In this chapter the development of the driver is described and divided into different main stages. The tools and techniques used to develop the driver are showed and explained.

### 3.1 Planning

During the first stage of the development process the requirements for the driver were specified. These requirements were specified in chapter 1.1 Design requirements.

According to the initial design plan a simple flow chart was constructed to help visualize the driver's working principle.

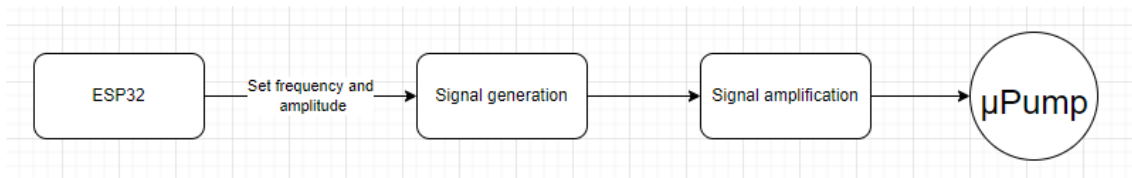


Figure 22. Initial design flow chart.

The design of the driver would have ESP32 as its MCU and would control the output frequency, amplitude and waveform. Inputs from the ESP32 would be used to generate the required waveform and then amplified to a high voltage required by the micropump.

### 3.2 Analysis and models

Various methods were researched and tested using simulation software LTspice after setting the driver requirements to determine which one would meet the required performance parameters. The simulation process allowed for the simulation of different driver designs and identification of potential issues with them. Signal generation and signal amplification were the two main parts of the driver that were modelled and tested in LTspice. After running and analysing different solutions, the most suitable design was selected.

A prototype design was constructed using the Analog Design AD9833 signal generator, four rail-to-rail op amps, and Microchip's HV264 quad opamp. The final output utilized Microchip's quad high voltage amplifier array, which has a gain of 66.7 and four signal



inputs. To increase the signal to 200 V, an input signal of at least 3 V was required. Since the AD9833 has a fixed output between 38-650 mV, an intermediate amplification was necessary. To phase shift the signals by 180°, an inverting opamp with a non-inverting positive reference voltage circuit was utilized, as polarity change was unnecessary. The intermediate amplification was accomplished using two inverting operational amplifiers with positive voltage references and two operational amplifiers with a non-inverting configuration. The piezoelectric micropump will be set up as a floating load, and it will be driven by four signals: two with zero phase shift and two with a 180° phase shift (Figure 24).

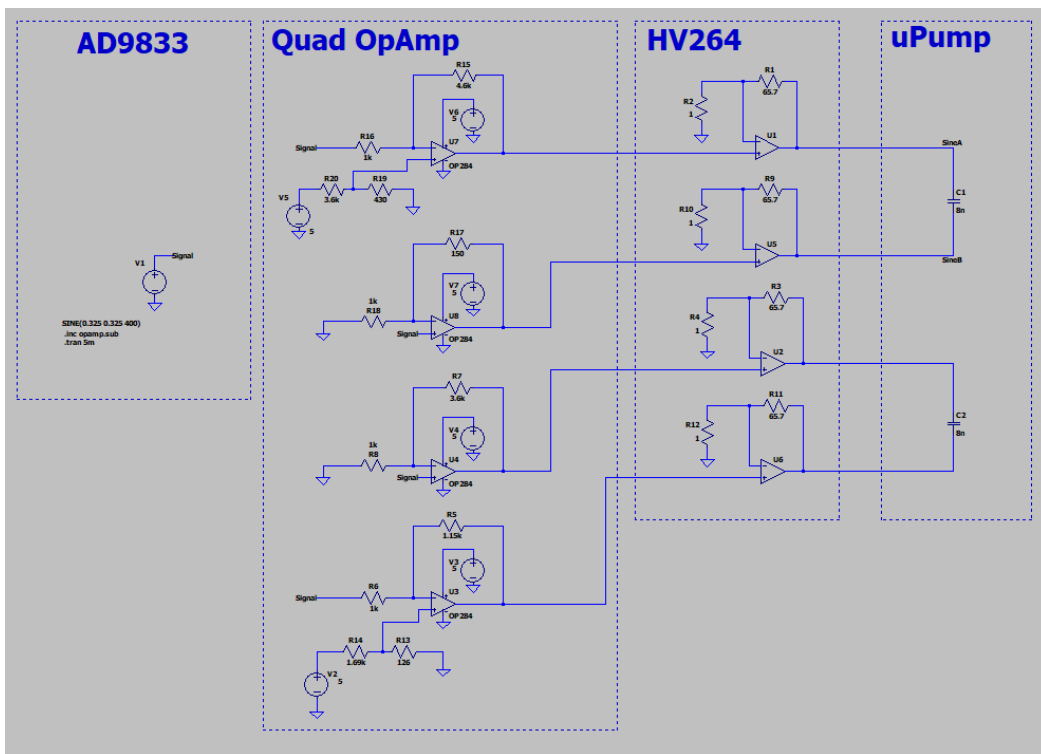


Figure 23. Prototype circuit in LTspice.

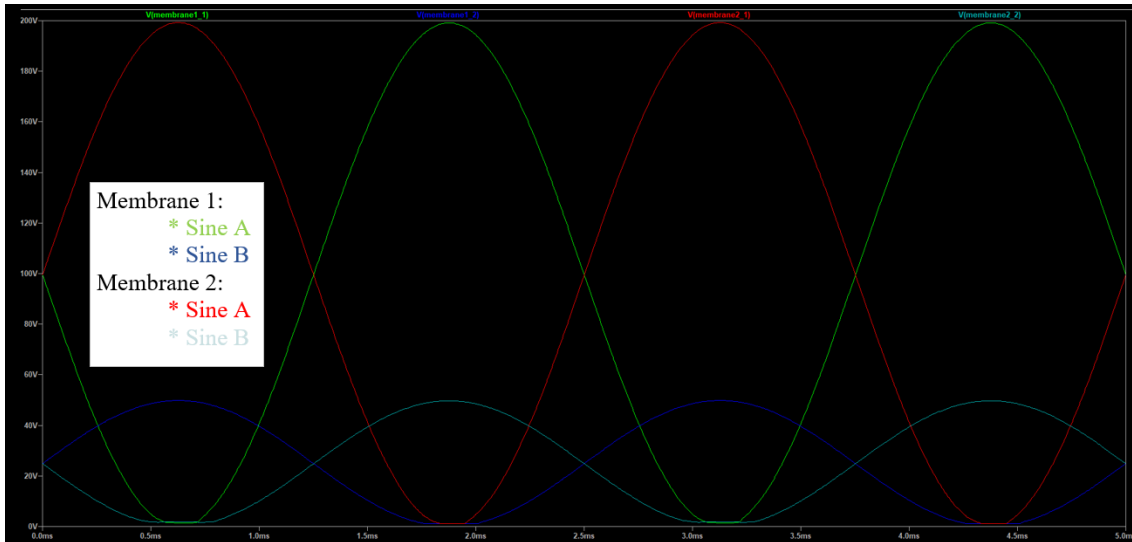


Figure 24. The waveforms of the signals supplied to the micropump.

Equations 3-5 were used to calculate the resistor values, to supply the correct voltage reference voltage divider equation was used (Equation 6).

$$V_{out} = \frac{V_{in} \cdot R_2}{R_1 + R_2} \quad (6)$$

A Microchip HV9150 was used to provide the necessary high voltage for amplification. This is a high-voltage hysteretic-mode Step-Up DC/DC controller, which was also featured in the Microchip application node demo [43].

### 3.3 Prototype board

The perforated board (DOT PCB) was used for building the prototype (Figure 25), which uncovered two design issues. Firstly, the signal output from AD9833 was distorted when supplied to four opamps. Secondly, there was no means of adjusting the signal amplitude. To address the distortion problem, an additional opamp was included as a buffer to prevent signal distortion. To enable amplitude modification, an Analog Design AD5144 digital potentiometer was added later. Despite these challenges, the prototype demonstrated that the solution is effective, and a basic test showed its ability to displace water using a micropump.

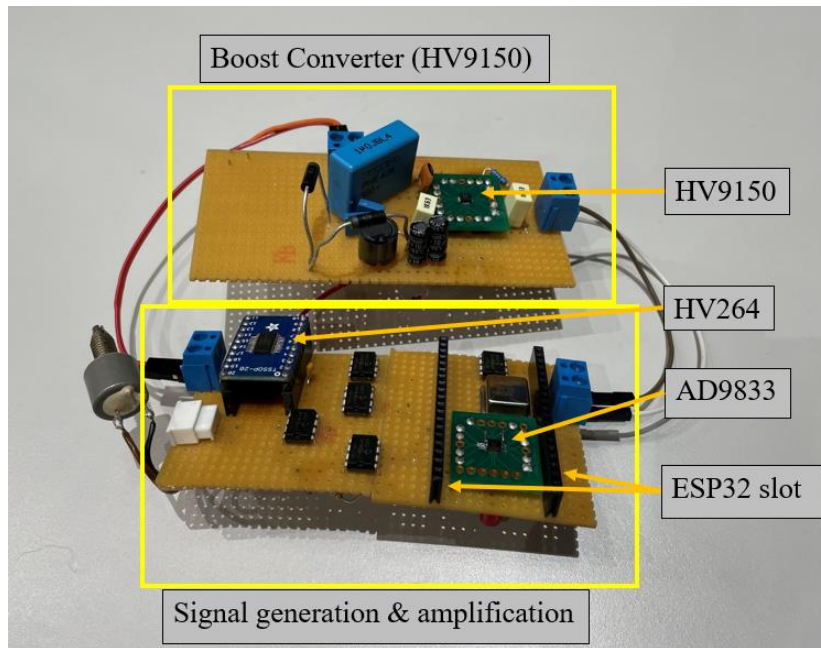


Figure 25. Prototype board.

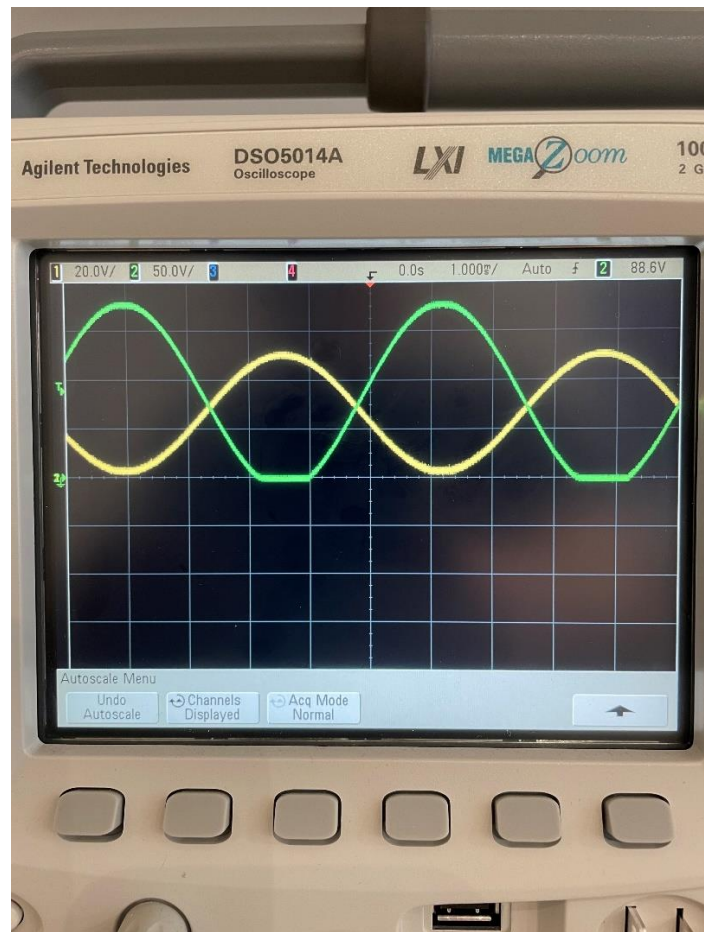


Figure 26. The output of the prototype while the micropump was connected and pumping.

### 3.4 Designing the PCB

Altium Designer software was used to create and develop both the schematics and the PCB. Compared to the prototype, the TLV9001 rail-to-rail opamp and AD5144 digital potentiometer were added (Figure 27). The PCB was designed to have two drivers on a single board, and an additional boost converter was included for comparison with the HV9150. The purpose of the additional boost converter is to serve as a testing platform for further development and to validate the parameters and functionality of the design. The traces were designed to be as short as possible to maintain signal integrity, while components were placed as close as possible to the IC while still providing comfortable distances to allow easier soldering. Figure 28 shows the final design outcome.

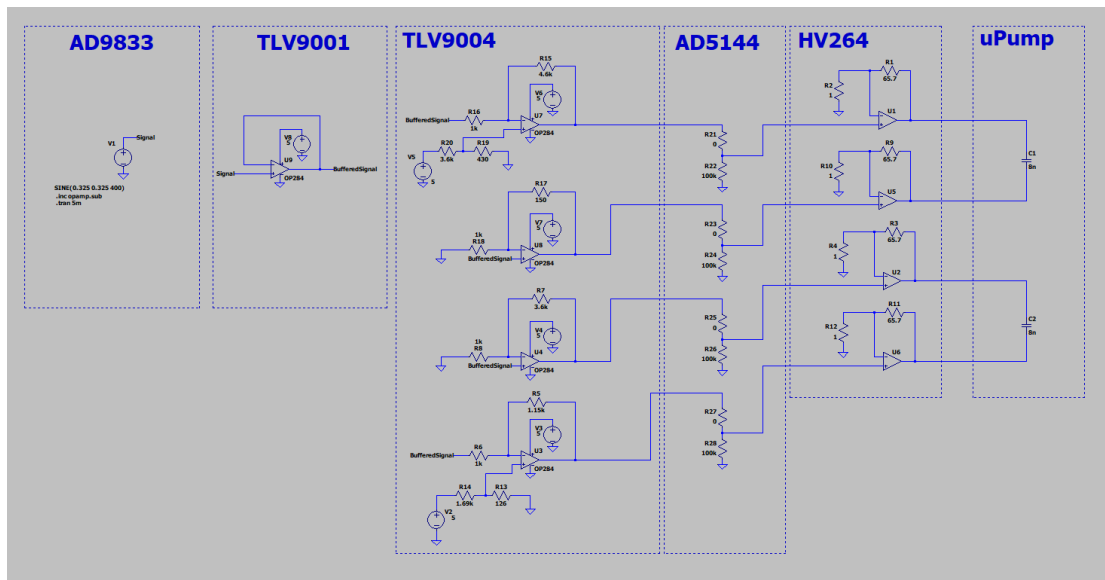


Figure 27. Final design in LTspice.

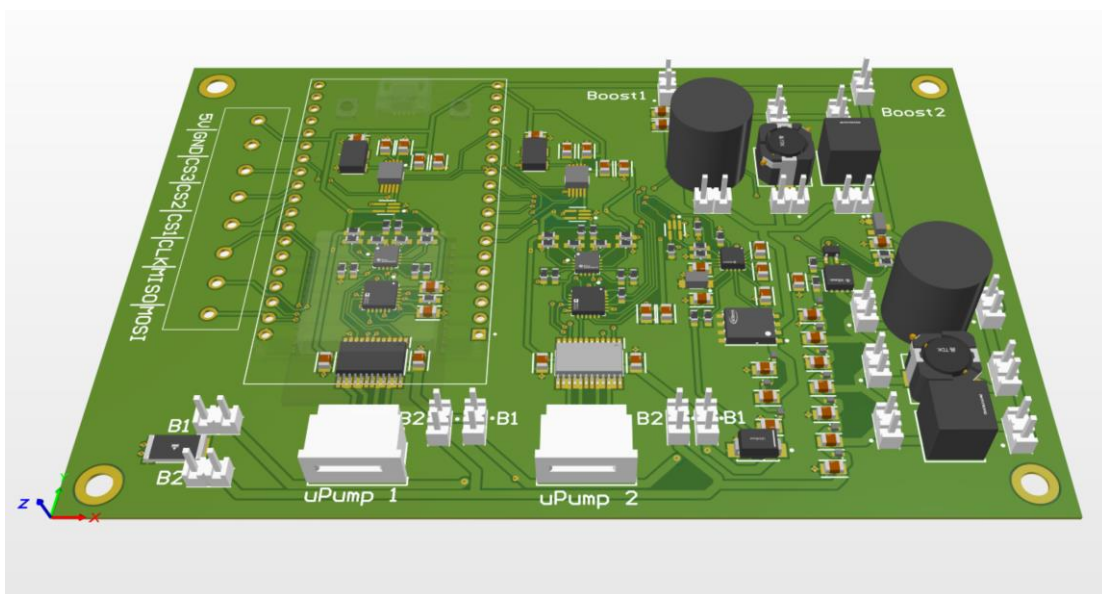


Figure 28. 3D model of the final PCB design.

## 4 Experimental analysis

Several measurements were carried out to evaluate the driver's performance. These measurements aimed to showcase the driver's three main properties, namely frequency, amplitude, and waveforms. Honeywell MPRLS0015PG0000SA piezoresistive silicon pressure sensor [47] was used to measure pressure, while Agilent DSO5014A oscilloscope [48] was used to measure frequency and voltage. Frequency was tested by fixing the output voltage to the maximum and changing the frequency. Amplitude was tested by fixing the frequency to the value that gave maximum pressure and changing the values on the digital potentiometer that altered the output voltage. Three different waveforms were tested, namely sine, square, and triangle. The tests were performed on both water and oil, except for the waveform test. During the measurements, the four driving signals will be labelled as high side 1, low side 1, high side 2, and low side 2 (Figure 29).

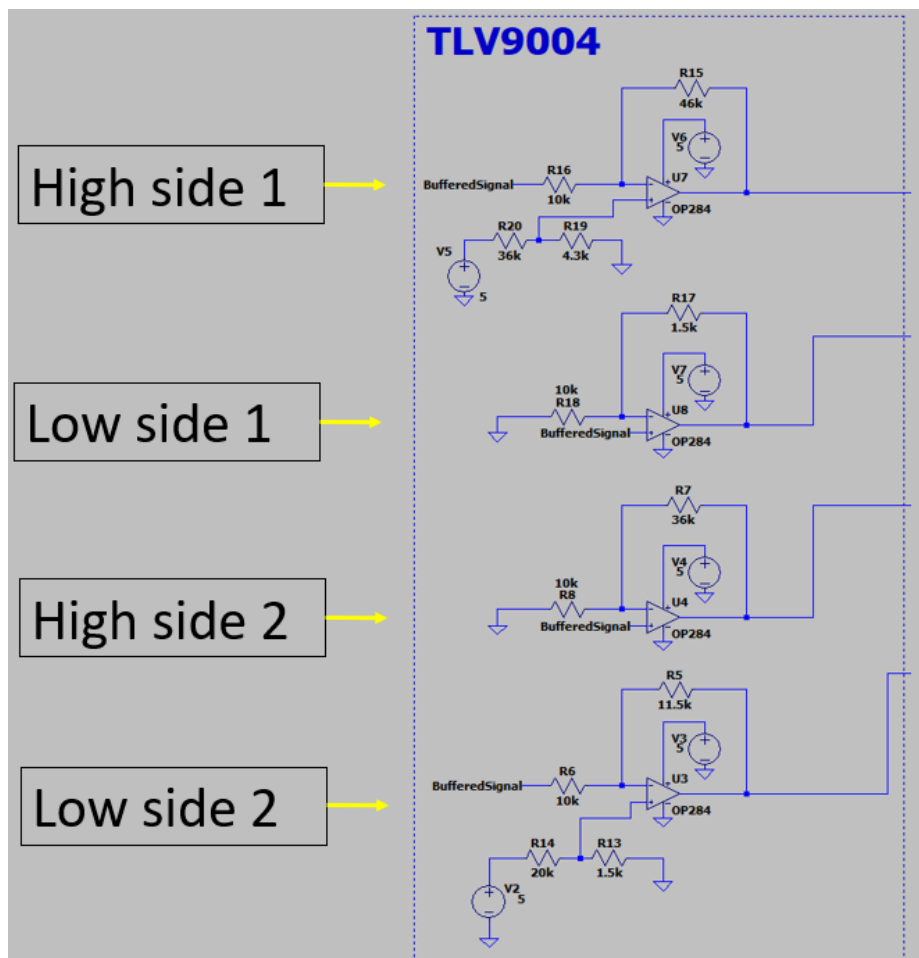


Figure 29. Driving signal labelling.

Two main parameters were measured, peak-to-peak values of the signals and the pressure created by the pump. Throughout the measurements the PWM frequency and duty cycle were constant. The PWM frequency was set at 50 kHz and the duty cycle at 94.53%. The digital potentiometer values were constant throughout frequency measurements but varied for others.

The noninverting input for high side 1 and low side 2 use a positive voltage reference that is provided through a voltage divider. However, due to the resistors not being 100% precise, the output may deviate from the desired outcome. To address this issue, measurements were conducted, which showed that low side 1 and high side 2 need to be around 5-6% lower to achieve the correct output. Throughout all the measurements, the peak-to-peak amplitude of the sine driving signals varied by only  $\mp 2$  V (Figure 30).

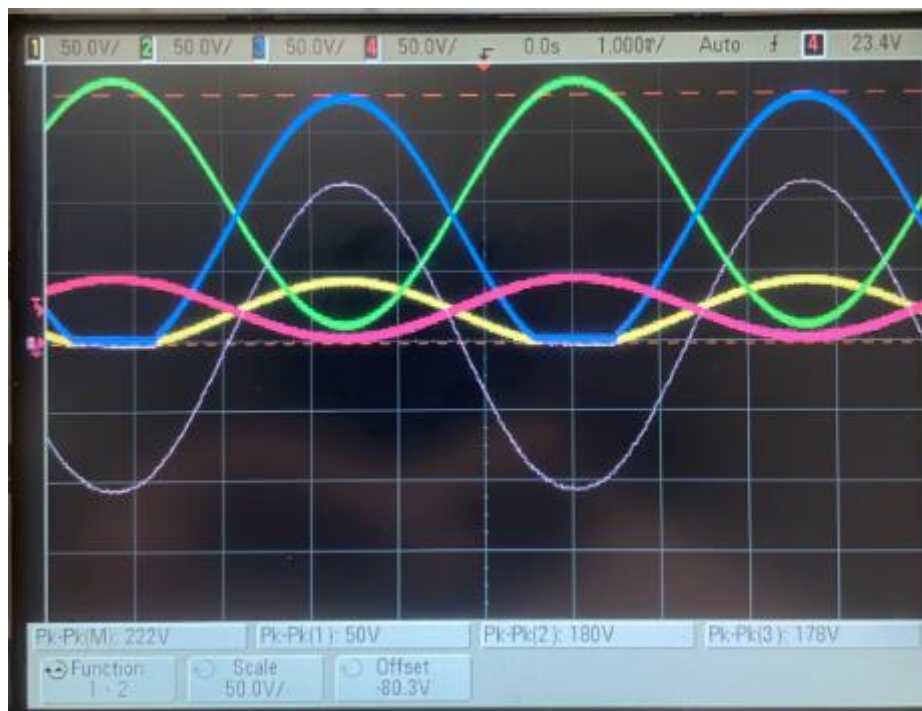


Figure 30. Peak-to-peak amplitude values at maximum output and at 200 Hz.

#### 4.1 Frequency measurements with distilled water

In total, 13 measurements with different frequencies were made (Figure 31). With the three highest average pressure shown on Figure 32. During the measurements the amplitude remained constant, with high side 1 and 2 at 180 V and low side 1 and 2 at 50 V. The digital potentiometer values are shown on Table 3, the figures are the percentage of the maximum output of the driver.

Table 3. Digital potentiometer values for varying frequency.

HighSide1	LowSide1	HighSide2	LowSide2
100%	94.53%	94.53%	100%

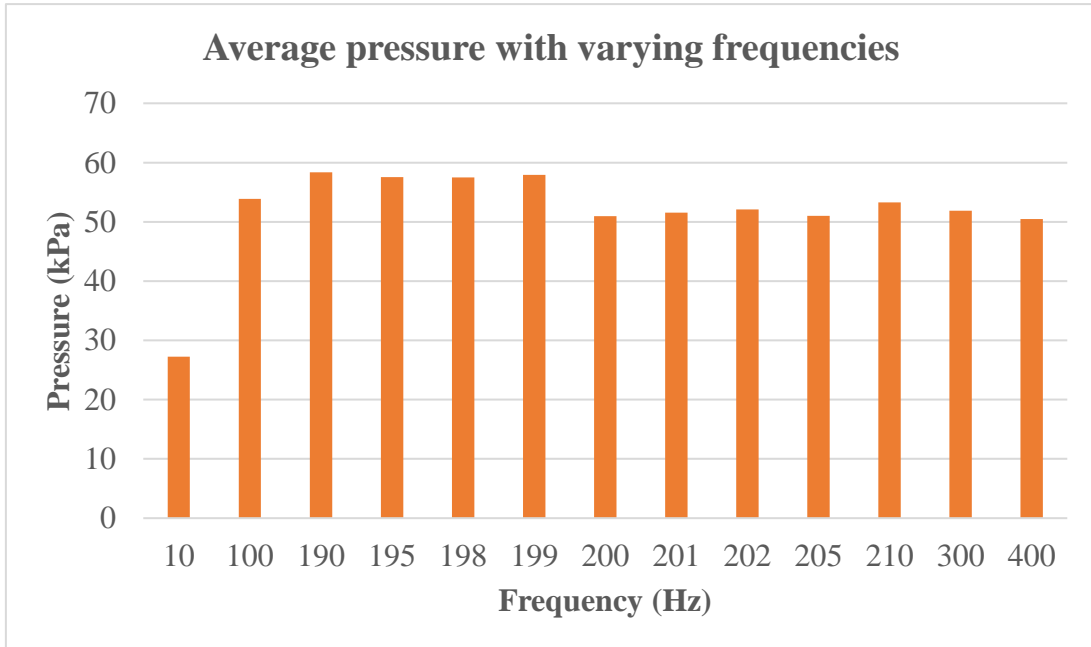


Figure 31. Average pressures with varying frequencies.

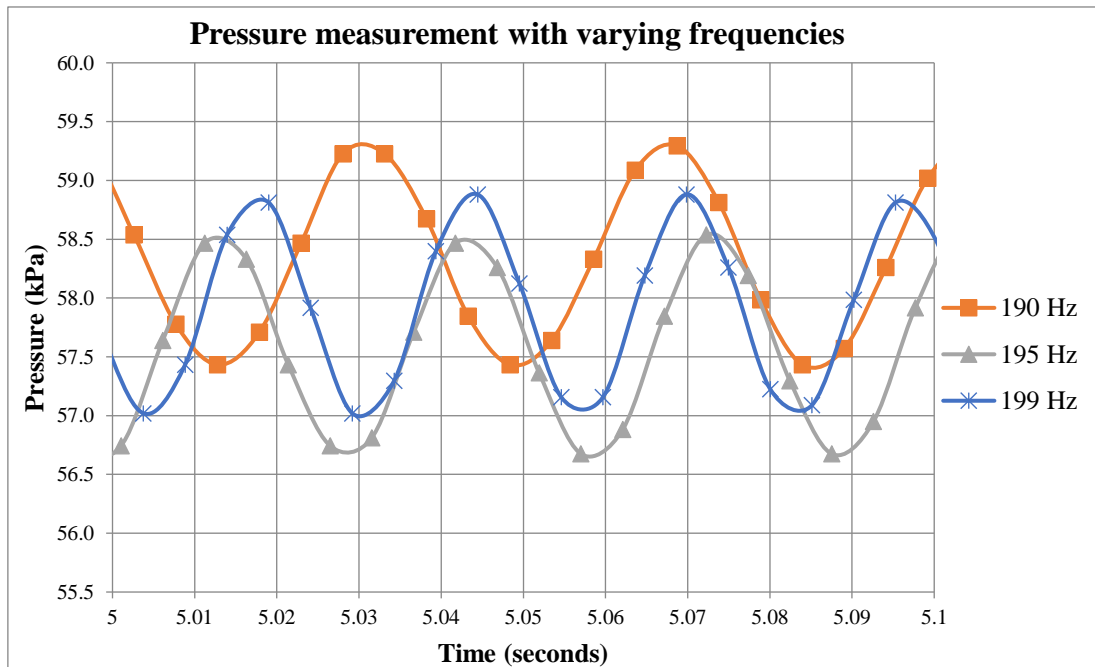


Figure 32. Three highest average pressure frequencies.



## 4.2 Amplitude measurements with distilled water

In order to demonstrate varying amplitudes, the frequency was set to 190 Hz and adjustments were made to the digital potentiometer values. The resulting average pressure over different voltages is presented on Figure 33.

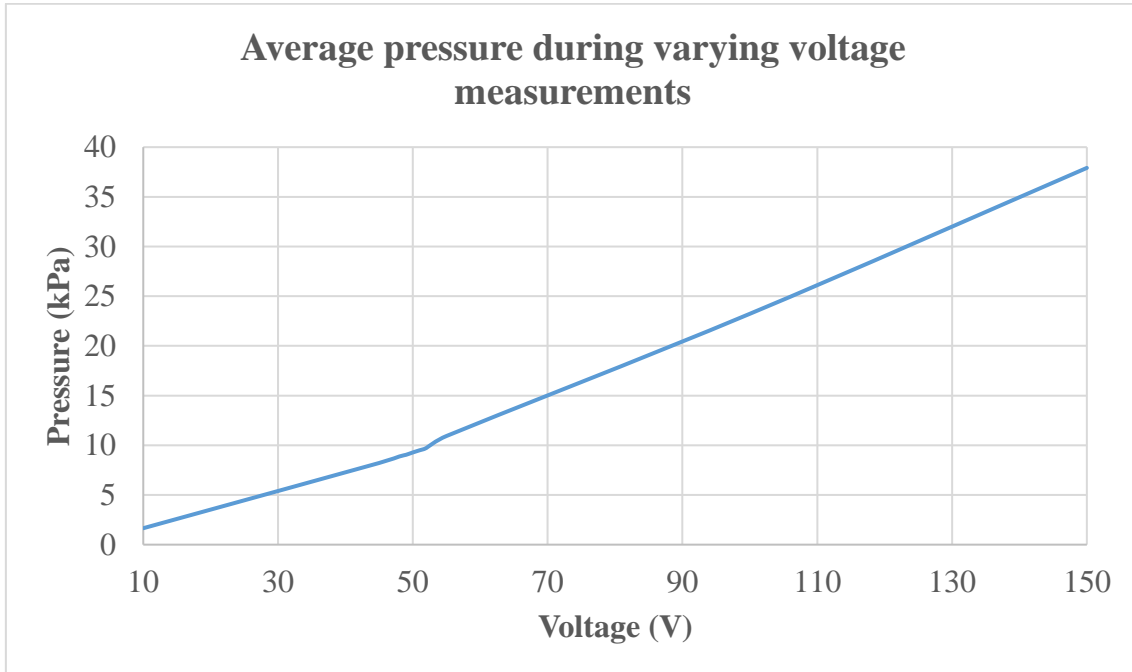


Figure 33. Average pressure during varying voltage measurements.

The input values for the potentiometer are given as percentages of the maximum output value on Table 4.

Table 4. Digital potentiometer values during varying voltage measurements.

Voltage	HighSide1	LowSide1	HighSide2	LowSide2
150	67%	63%	63%	67%
100	45%	42%	42%	45%
55	25%	23%	23%	25%
52	23%	21%	21%	23%
51	22%	21%	21%	22%
50	22%	21%	21%	22%
49	21%	20%	20%	21%
48	21%	20%	20%	21%
45	20%	19%	19%	20%



10	4%	4%	4%	4%
----	----	----	----	----

The peak-to-peak voltage values during the test are shown in Table 5.

Table 5. Peak-to-peak values during varying amplitude measurements.

Voltage	HighSide1 (V)	LowSide1 (V)	HighSide2 (V)	LowSide2 (V)
150	125	33	125	33
100	85	23.1	85	23.1
55	49	13.8	49	13.8
52	47	13.1	47	13.1
51	45	12.5	45	12.5
50	44	12.5	44	12.5
49	44	11.9	44	11.9
48	43	11.9	43	11.9
45	41	11.9	41	11.9
10	13	4.4	13	4.4

### 4.3 Waveform measurements with distilled water

Three different waveforms were tested, sine, triangle and square wave. All three were tested at 50, 150 and 220 V and at 190 Hz (Figure 34).

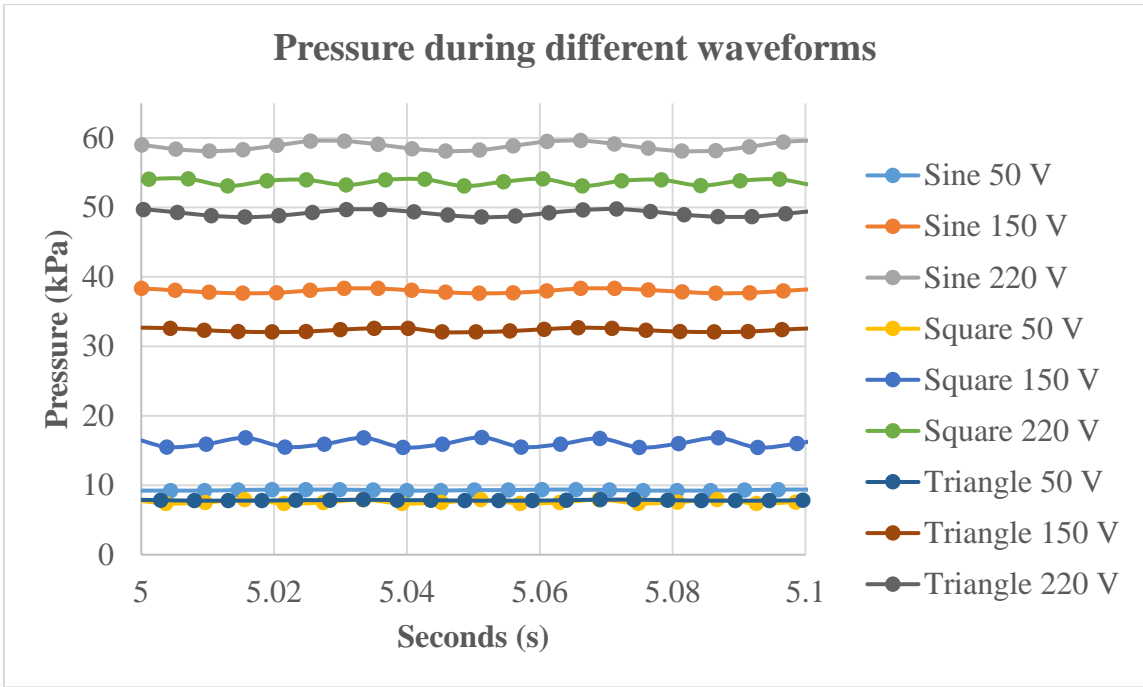


Figure 34. Pressure during varying waveform measurements.

The potentiometer values are shown as percentages from the maximum output in Table 6.

Table 6. Digital potentiometer values during varying waveform measurements.

Waveform	Voltage	High side 1	Low side 1	High side 2	Low side 2
Sine	50	22%	21%	21%	22%
	150	67%	63%	63%	67%
	220	100%	94%	94%	100%
Square	50	14%	13%	13%	14%
	150	43%	40%	40%	43%
	247	100%	94%	94%	100%
Triangle	50	23%	21%	21%	23%
	150	69%	65%	65%	69%
	217	100%	94%	94%	100%

The voltage values during different waveform measurements are shown on Table 7.

Table 7. Voltage values during varying waveform measurements.

Waveform	Voltage	High side 1	Low side 1	High side 2	Low side 2
Sine	50	44	12.5	44	12.5
	150	123	32.5	123	32.5

	220	181	50	181	50
Square	50	28	20	28	5
	150	90	59	90	17
	247	135.9	139.5	143.5	39.2
Triangle	50	45	15	45	15
	150	127	34	127	34
	217	180	50	180	50

The values for the square wave measurements were abnormal (Table 7). This may be due to the boost converter not being able to supply enough power. The sudden transition in a square wave may exceed the converters capacity, resulting in a voltage drop. In the appropriate handling document by Bartels Mikrotechnik [49], it is noted that square wave signals should only be used for brief periods to avoid potential pump malfunction (Figure 35).

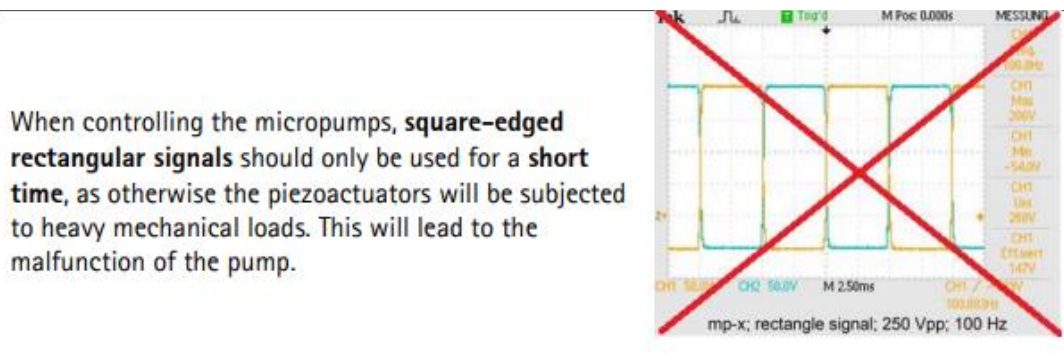


Figure 35. Instruction for appropriate handling [49].

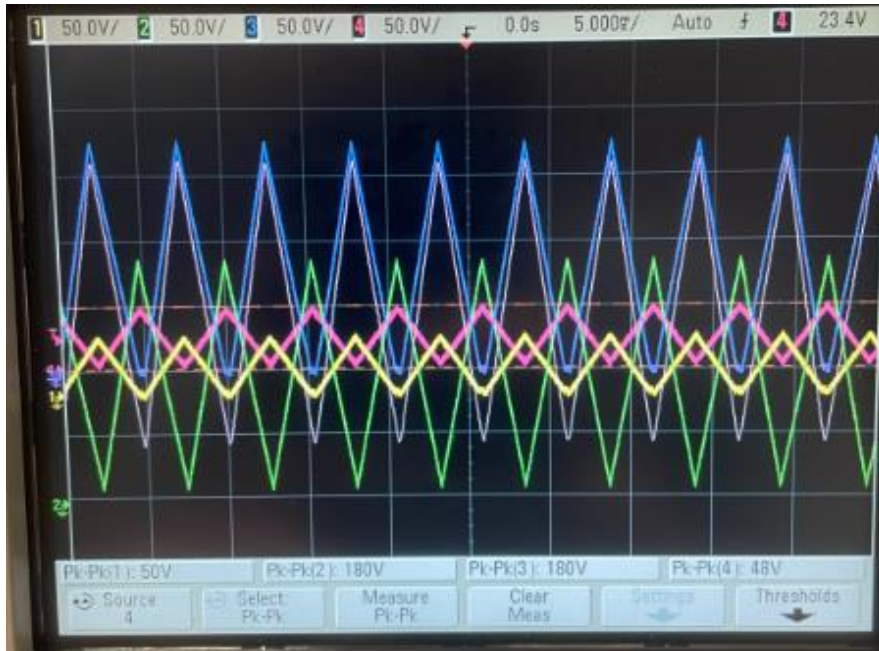


Figure 36. Peak-to-peak triangle wave amplitude values at 190 Hz.

#### 4.4 Frequency measurements with oil

The oil used for the measurements was mineral oil with 2% w/w surfactant (Span® 80, Sigma-Aldrich). Ten different measurements with varying frequencies were made (Figure 37). With the three highest average pressure shown on Figure 38. During the measurements the amplitude remained constant, with high side 1 and 2 at 180 V and low side 1 and 2 at 50 V. The digital potentiometer values were same as for distilled water, shown on Table 3.

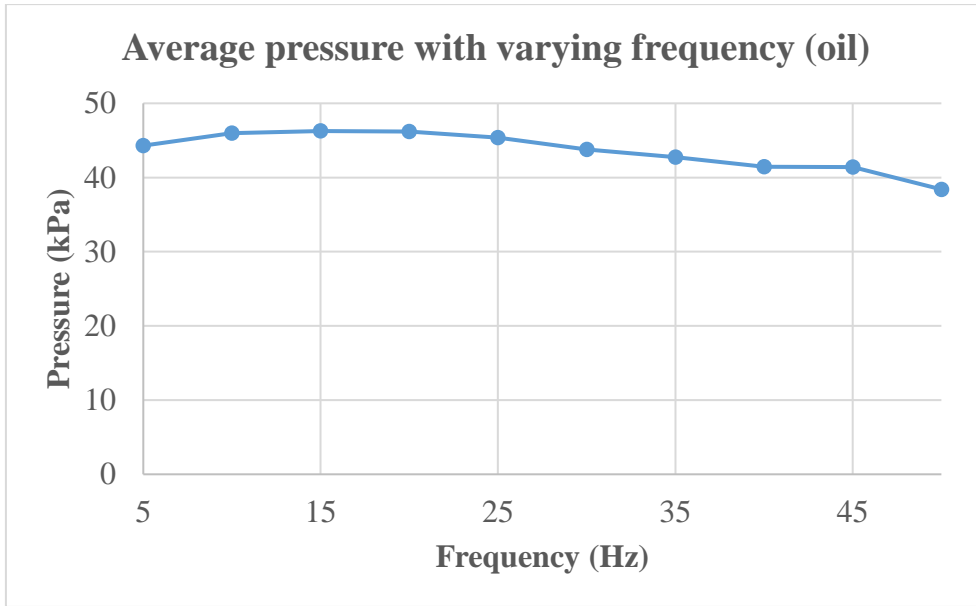


Figure 37. Average pressure during varying frequency measurements with oil.

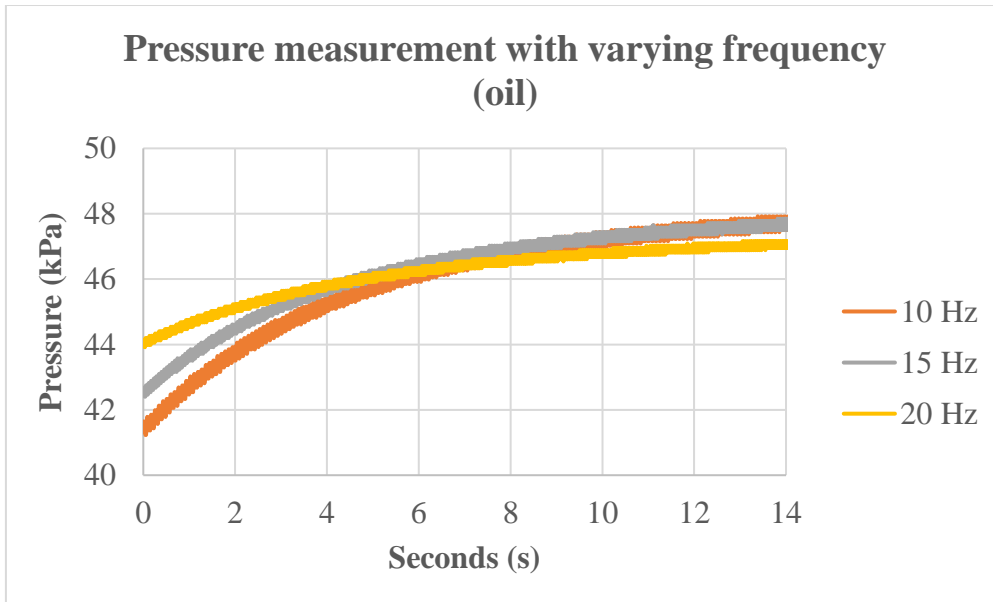


Figure 38. Three highest average pressure frequency (oil).

#### 4.5 Amplitude measurements with oil

Amplitude measurements were conducted at 10 Hz, a sine wave was used to drive the signal. In total, 12 measurements were made (Figure 39).

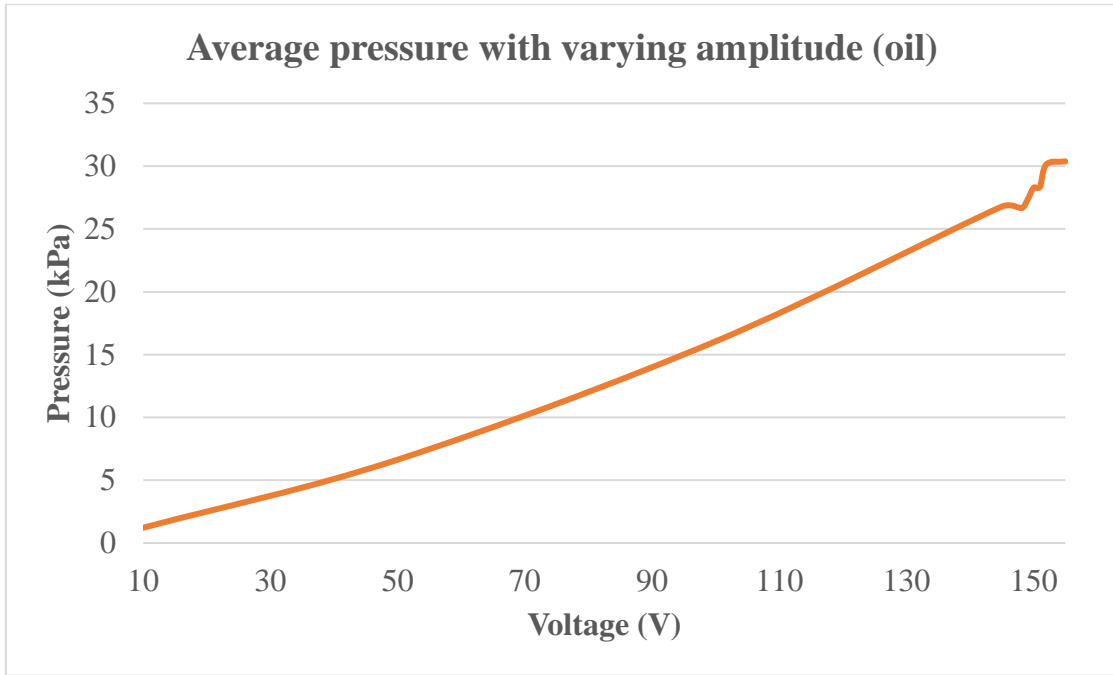


Figure 39. Average pressure with varying amplitude (oil)

The input values for the potentiometer are given as percentages of the maximum output value on Table 8.

Table 8. Digital potentiometer values during varying amplitude measurements (oil).

Voltage	HighSide1	LowSide1	HighSide2	LowSide2
155	70%	66%	66%	70%
152	68%	64%	64%	68%
151	68%	64%	64%	68%
150	67%	63%	63%	67%
149	67%	63%	63%	67%
148	66%	63%	63%	66%
145	65%	61%	61%	65%
100	45%	42%	42%	45%
50	22%	21%	21%	22%
10	5%	5%	5%	5%

Table 9. Voltage values during varying amplitude measurements (oil).

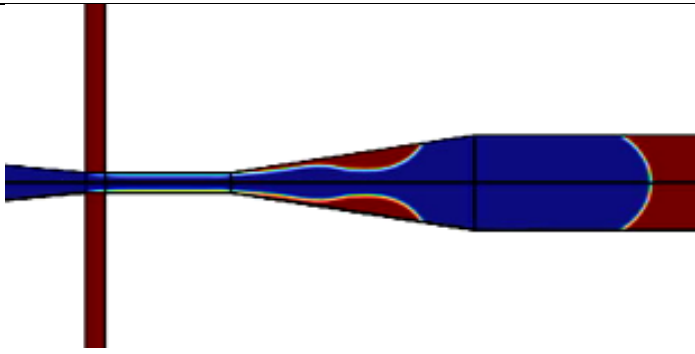
Voltage	HighSide1 (3)	LowSide1 (4)	HighSide2 (2)	LowSide2 (1)
155	128	36	128	36

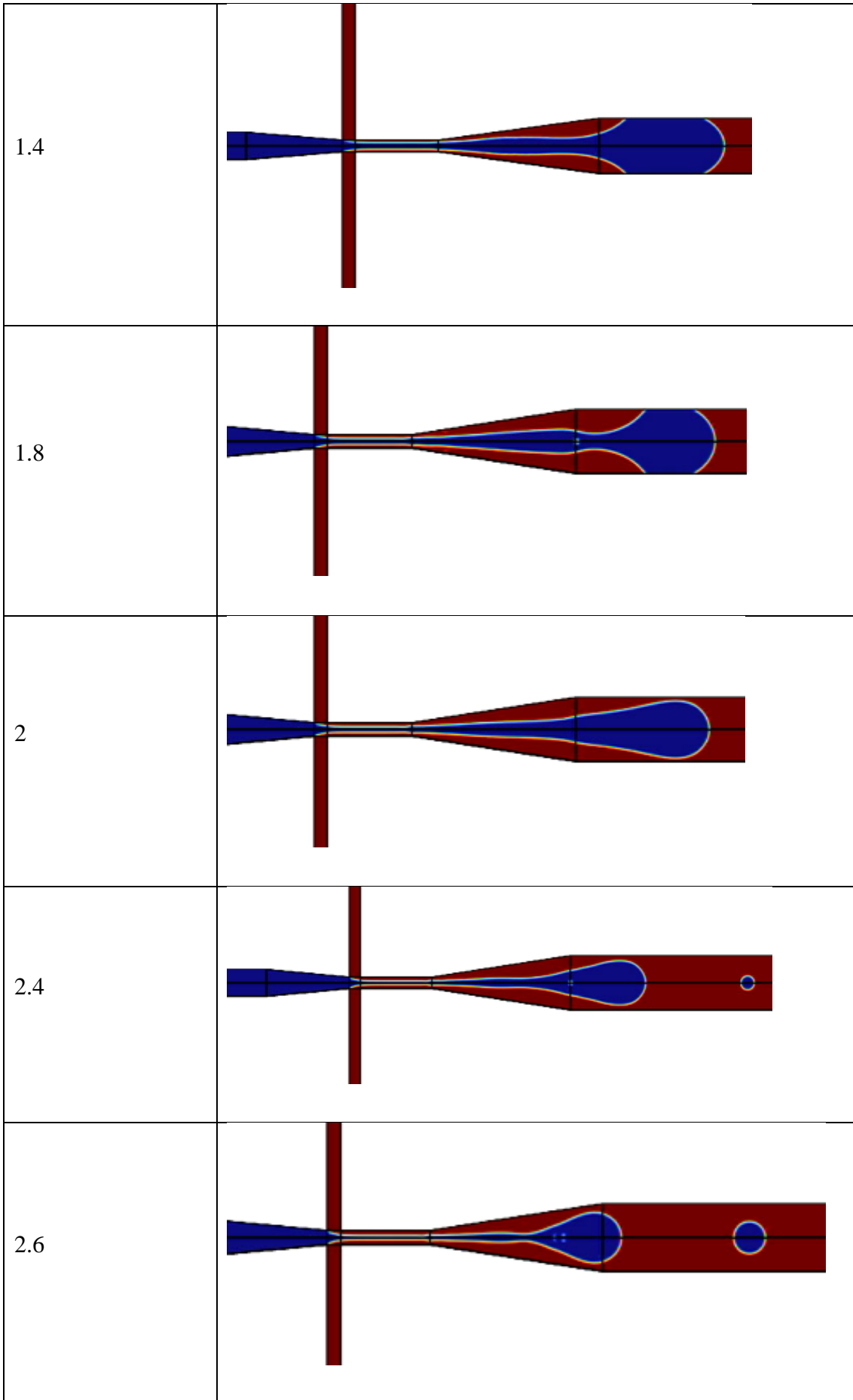
152	125	36	125	36
151	124	36	124	36
150	123	36	123	36
149	122	35	122	35
148	122	34	122	34
145	119	34	119	34
100	83	25	83	25
50	44	16	44	16
10	9.7	2.5	9.7	2.5

#### 4.6 Droplet generation simulations

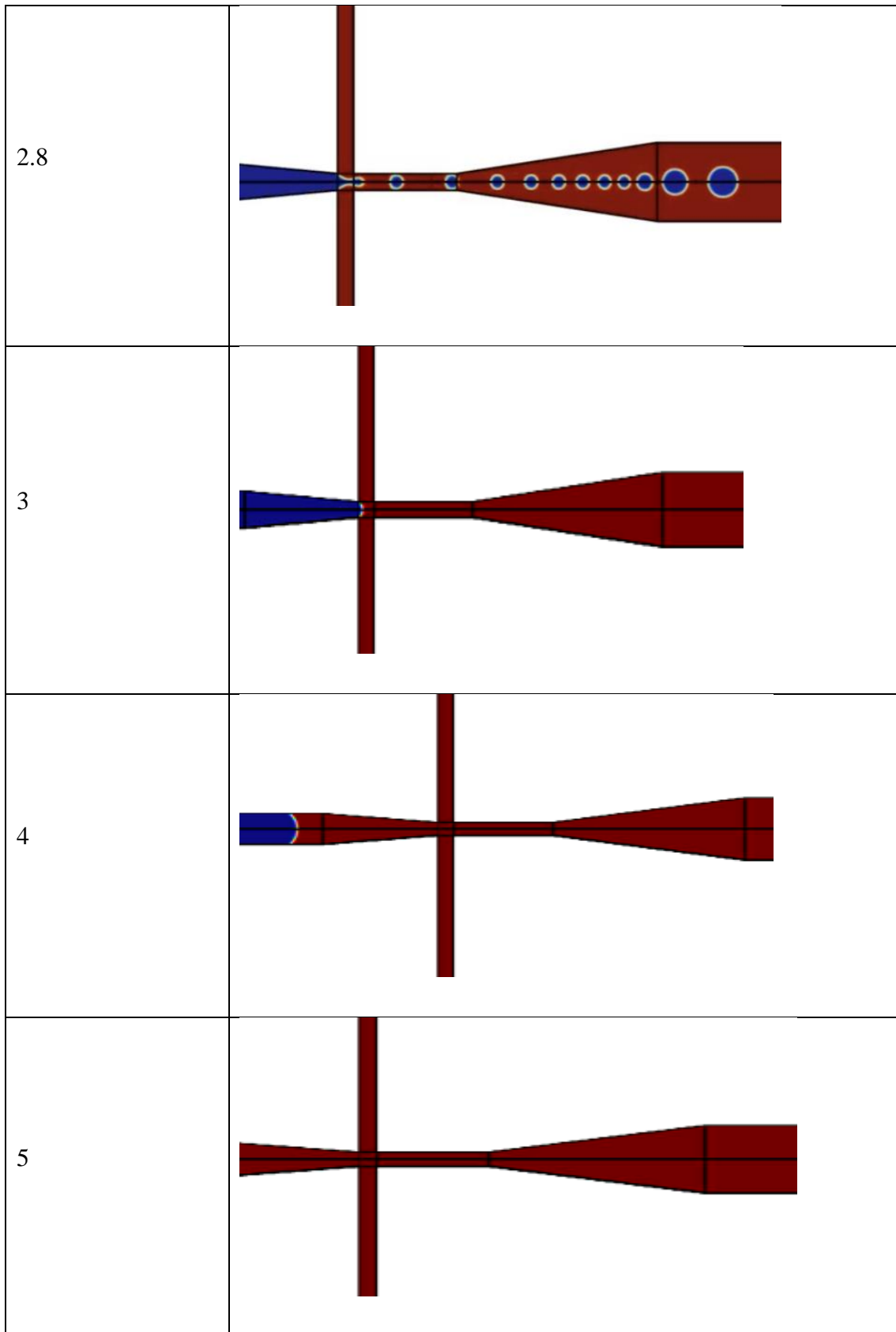
The COMSOL Multiphysics software was used to simulate and determine the necessary pressure conditions for droplet generation. A paper was published on the model used, which explains in detail how it works [50]. A total of 21 different sets were simulated over a duration of 0.15 seconds, with 10 of those shown in Table 10. The computational time required to generate these outputs was about 3.5 hours.

Table 10. Droplet generation simulation results from COMSOL

$p_{oil} / p_{water}$	Result (blue = water phase, red = oil phase)
1	







Based on the results, it was observed that the optimal condition for droplet generation occurs when the water to oil to water ratio is 2.8 (Table 10). The measurements conducted

with distilled water and oil indicated that the driver could generate approximately 20% higher pressure with distilled water compared to oil. However, it is still possible to achieve a ratio of 2.8 using this driver, which demonstrates its capability to generate sufficient pressure for droplet generation.

#### 4.7 Comparison to existing driver

To provide a reference point for comparison, pressure data was gathered from the datasheet of the Bartels Mikrotechnik mp6 micropump [29], where an mp-Highdriver was used for pressure measurements (Figure 40). Pressure measurements were taken at 3 different frequencies and 3 different voltages, specifically at 50 V, 150 V, and 200 V. The pressure measurement data for the developed driver can be seen in Figure 41.

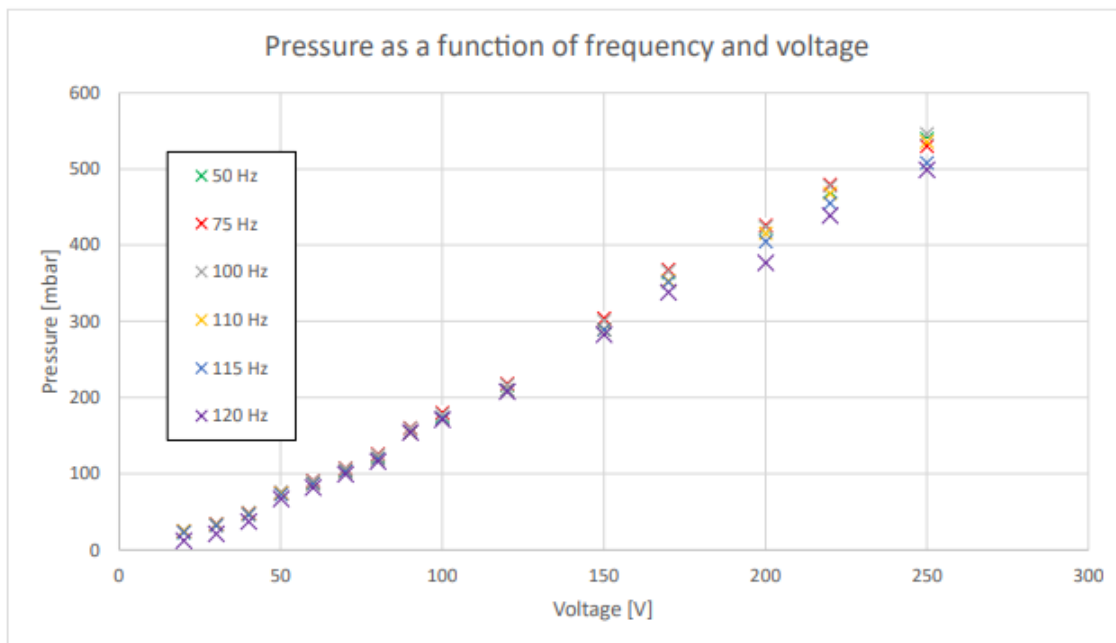


Figure 40. Bartels mikrotechnik mp-Highdriver pressure measurements [29].

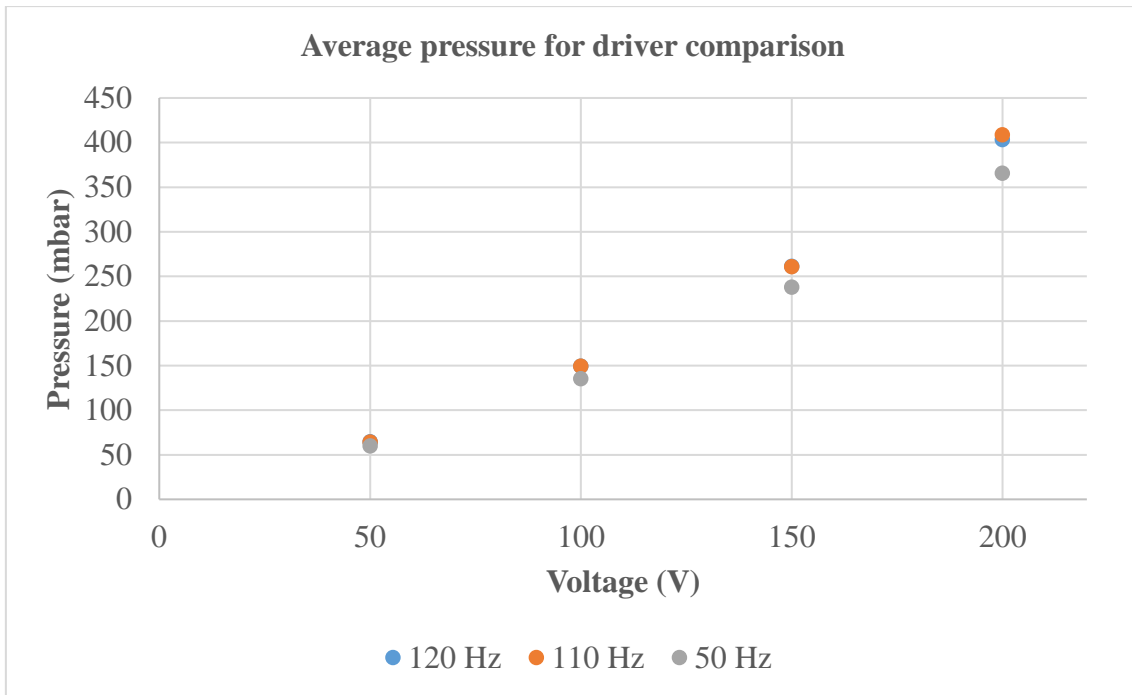


Figure 41. Average pressure measurements for driver comparison.

When comparing the two figures (Figure 40, Figure 41), it can be observed that the Bartels Mikrotechnik driver exhibits a slightly higher average pressure compared to the developed driver. However, it should be noted that the exact test setup details (such as the pressure sensor used and the length of the tubes) are not specified in the datasheet. Therefore, the actual performance difference may vary from what is shown here. Nevertheless, based on the available data, the performance of the developed driver falls within the same range as an existing driver on the market.

## **5 Future developments**

### **5.1 Next iteration PCB**

In the next iteration of the PCB design, the PCB should host only one driving circuit and boost converter. This change would result in a smaller-sized PCB with several advantages, including cost reduction, space optimization, and improved efficiency. Combining the two driving circuits into one will reduce the overall component count and simplify the PCB layout. Additionally, a smaller PCB size often results in improved electrical performance. It reduces parasitic capacitance and inductance, leading to enhanced signal integrity.

### **5.2 Create library/GUI for driver**

Developing a dedicated library and/or graphical user interface (GUI) for the driver would greatly enhance the user experience and simplify the usage of the driver. One key improvement would be to provide real-time feedback to the user, eliminating the need for external measurement systems such as oscilloscopes or multimeters.

By integrating feedback mechanisms into the library/GUI, users can receive immediate information about the driver's performance and functionality. This can include visual indicators, status messages, and graphical representations of key parameters such as voltage, frequency, and waveform. The user will be able to monitor the driver's operation and ensure it is functioning correctly without the need for additional measurement tools.

### **5.3 Add output voltage and boost converter feedback**

Currently, the system lacks feedback for the output voltage. To address this limitation, a recommended future development is to integrate an output voltage feedback mechanism. This addition would enable continuous monitoring of the actual output voltage, allowing for real-time comparison with the desired voltage. By using this feedback information, the driver can dynamically adjust the driving signal to ensure the output voltage remains within the desired range, even when faced with load variations or external influences. Implementing output voltage feedback would greatly enhance the precision and stability

of the driver, ultimately leading to improved performance and increased reliability of the entire system.

## 6 Summary

The goal of this thesis was to develop a customized piezoelectric pump driver, that could be used for droplet generation in TalTech project PRG620.

The presented work explored various potential solutions for driver development and provided an overview of existing options. In the end, a driver was successfully developed, capable of generating a wide range of frequencies, amplitudes, and multiple waveforms. The driver incorporates signal generation, first-stage amplification, amplitude control, and second-stage amplification powered by a boost converter.

The development process involved four main stages: planning, analysing solutions and creating models, building a prototype board on a dot PCB, and finally designing a dedicated PCB.

The driver's parameters were tested and measured using both distilled water and oil. The results indicated that the driver could generate pressures suitable for droplet generation.

Furthermore, a comparison was conducted between the developed driver and an existing piezoelectric driver, demonstrating that the developed driver operates within the same pressure range.

For future development, three key suggestions were proposed. Firstly, reducing the size of the PCB to enhance signal integrity. Secondly, creating a library/GUI for the driver to enhance usability. Lastly, incorporating voltage and boost converter feedback to improve system stability.

Overall, the developed driver successfully fulfils the initial design requirements, showcasing its effectiveness and potential for further advancements.

## References

- [1] S.-M. Yang, S. Lv, W. Zhang, and Y. Cui, ‘Microfluidic Point-of-Care (POC) Devices in Early Diagnosis: A Review of Opportunities and Challenges’, *Sensors*, vol. 22, no. 4, p. 1620, Feb. 2022, doi: 10.3390/s22041620.
- [2] J. M. Ayuso, M. Virumbrales-Muñoz, J. M. Lang, and D. J. Beebe, ‘A role for microfluidic systems in precision medicine’, *Nat. Commun.*, vol. 13, no. 1, Art. no. 1, Jun. 2022, doi: 10.1038/s41467-022-30384-7.
- [3] Elveflow, ‘White paper droplet based microfluidics Elveflow microfluidics’. <https://www.elveflow.com/wp-content/uploads/2019/12/White-paper-droplet-based-microfluidics-Elveflow-microfluidics.pdf> (accessed Apr. 09, 2023).
- [4] S.-Y. Teh, R. Lin, L.-H. Hung, and A. P. Lee, ‘Droplet microfluidics’, *Lab. Chip*, vol. 8, no. 2, pp. 198–220, 2008, doi: 10.1039/B715524G.
- [5] ‘Introduction to droplet-based microfluidics’, *Elveflow*. <https://www.elveflow.com/microfluidic-reviews/droplet-digital-microfluidics/introduction-to-droplet-based-microfluidics/> (accessed Apr. 09, 2023).
- [6] P. Zhu and L. Wang, ‘Passive and active droplet generation with microfluidics: a review’, *Lab. Chip*, vol. 17, no. 1, pp. 34–75, 2017, doi: 10.1039/C6LC01018K.
- [7] Z. Z. Chong, S. H. Tan, A. M. Gañán-Calvo, S. B. Tor, N. H. Loh, and N.-T. Nguyen, ‘Active droplet generation in microfluidics’, *Lab. Chip*, vol. 16, no. 1, pp. 35–58, 2016, doi: 10.1039/C5LC01012H.
- [8] ‘Lab on a Chip | TalTech’, Jan. 22, 2020. <https://taltech.ee/en/labonchip> (accessed May 01, 2023).
- [9] E. Team, ‘Introduction to lab-on-a-chip 2020: review, history and future’, *Elveflow*, Feb. 2021, Accessed: Dec. 04, 2022. [Online]. Available: <https://www.elveflow.com/microfluidic-reviews/general-microfluidics/introduction-to-lab-on-a-chip-review-history-and-future/>
- [10] ‘Lab-on-a-chip for tracking single bacterial cells - EPR’, *European Pharmaceutical Review*. <https://www.europeanpharmaceuticalreview.com/news/72373/lab-on-a-chip-bacterial-cells/> (accessed Jan. 09, 2023).
- [11] F. Bragheri, R. Martínez Vázquez, and R. Osellame, ‘Chapter 12.3 - Microfluidics’, in *Three-Dimensional Microfabrication Using Two-Photon Polymerization (Second Edition)*, T. Baldacchini, Ed., in Micro and Nano Technologies. William Andrew Publishing, 2020, pp. 493–526. doi: 10.1016/B978-0-12-817827-0.00057-6.
- [12] J. Novotný and F. Foret, ‘Fluid manipulation on the micro-scale: Basics of fluid behavior in microfluidics’, *J. Sep. Sci.*, vol. 40, no. 1, pp. 383–394, Jan. 2017, doi: 10.1002/jssc.201600905.
- [13] G. M. Whitesides, ‘The origins and the future of microfluidics’, *Nature*, vol. 442, no. 7101, Art. no. 7101, Jul. 2006, doi: 10.1038/nature05058.

- [14] S. Momeniazandariani, ‘Chemical synthesis with microfluidics – a review’, *Elveflow*, Jun. 2022, Accessed: Apr. 30, 2023. [Online]. Available: <https://www.elveflow.com/microfluidic-reviews/general-microfluidics/chemical-synthesis-with-microfluidics-review/>
- [15] E. Team, ‘Microfluidics for DNA analysis’, *Elveflow*, Feb. 2021, Accessed: Apr. 30, 2023. [Online]. Available: <https://www.elveflow.com/microfluidic-reviews/general-microfluidics/microfluidics-for-dna-analysis-pcr/>
- [16] N.-T. Nguyen, S. T. Wereley, and S. A. M. Shaegh, *Fundamentals and Applications of Microfluidics, Third Edition*. Artech House, 2019.
- [17] ‘Immiscible Liquids and Steam Distillation’, *Chemistry LibreTexts*, Oct. 03, 2013. [https://chem.libretexts.org/Bookshelves/Physical\\_and\\_Theoretical\\_Chemistry\\_Textbook\\_Maps/Supplemental\\_Modules\\_\(Physical\\_and\\_Theoretical\\_Chemistry\)/Equilibria/Physical\\_Equilibria/Immiscible\\_Liquids\\_and\\_Steam\\_Distillation](https://chem.libretexts.org/Bookshelves/Physical_and_Theoretical_Chemistry_Textbook_Maps/Supplemental_Modules_(Physical_and_Theoretical_Chemistry)/Equilibria/Physical_Equilibria/Immiscible_Liquids_and_Steam_Distillation) (accessed Apr. 09, 2023).
- [18] ‘Digital microfluidics: microfluidic droplet and emulsion science’, *Elveflow*. <https://www.elveflow.com/microfluidic-reviews/droplet-digital-microfluidics/digital-microfluidics-microfluidic-droplet-emulsion-science/> (accessed Apr. 09, 2023).
- [19] S. L. Anna, N. Bontoux, and H. A. Stone, ‘Formation of dispersions using “flow focusing” in microchannels’, *Appl. Phys. Lett.*, vol. 82, no. 3, pp. 364–366, Jan. 2003, doi: 10.1063/1.1537519.
- [20] ‘Figure 6. Droplet production in the flow-focusing junction.’, *ResearchGate*. [https://www.researchgate.net/figure/Droplet-production-in-the-flow-focusing-junction\\_fig5\\_278826711](https://www.researchgate.net/figure/Droplet-production-in-the-flow-focusing-junction_fig5_278826711) (accessed Apr. 09, 2023).
- [21] L. Labarre and T. E. Team, ‘microfluidic t junction’, *Elveflow*, May 2021, Accessed: Apr. 09, 2023. [Online]. Available: <https://www.elveflow.com/microfluidic-reviews/microfluidic-flow-control/microfluidic-t-junction/>
- [22] ‘Piezoelectricity - an overview | ScienceDirect Topics’. <https://www.sciencedirect.com/topics/materials-science/piezoelectricity> (accessed Oct. 12, 2022).
- [23] ‘Micropumps’, *Bartels Mikrotechnik GmbH*. <https://www.bartels-mikrotechnik.de/en/micropumps/> (accessed Oct. 12, 2022).
- [24] *Assembly mp6 Bartels Micropump | Bartels Mikrotechnik*, (Oct. 26, 2015). Accessed: May 06, 2023. [Online Video]. Available: <https://www.youtube.com/watch?v=U-N7sKdKTXQ>
- [25] F. Bartels, S. Dahms, U. Kampmeyer, and M. Rawert, ‘Verfahren zum fördern eines fluids und mikropumpe hierfür’, EP2222959B1, Jan. 25, 2012 Accessed: May 07, 2023. [Online]. Available: <https://patents.google.com/patent/EP2222959B1/en?q=VERFAHREN+ZUM+F%C3%96RDERN+EINES+FLUIDS+UND+MIKROPUMPE+HIERF%C3%96R++European+Patent+Office++EP+2222959+B1>
- [26] ‘microcontroller’, *Oxford Reference*. <https://> (accessed May 04, 2023).
- [27] ‘Motor Controller - an overview | ScienceDirect Topics’. <https://www.sciencedirect.com/topics/engineering/motor-controller> (accessed Oct. 12, 2022).
- [28] ‘Driver Design in Piezoelectric Motors | Mouser’. <https://www.mouser.de/applications/driver-design-in-piezoelectric-motors/> (accessed Apr. 09, 2023).



- [29] ‘Bartels Mikrotechnik, mp6 Micropumps Datasheet’. Accessed: Oct. 12, 2022. [Online]. Available: [https://www.bartels-mikrotechnik.de/wp-content/uploads/simple-file-list/EN/Manuals-and-Data-Sheets/mp6\\_micropumps\\_Datasheet.pdf](https://www.bartels-mikrotechnik.de/wp-content/uploads/simple-file-list/EN/Manuals-and-Data-Sheets/mp6_micropumps_Datasheet.pdf)
- [30] M. H. Rashid, ‘Power electronics: circuits, devices, and applications’, *Choice Rev. Online*, vol. 3, p. 584, 1989.
- [31] ‘Signals and signal processing | Elsevier Enhanced Reader’. <https://reader.elsevier.com/reader/sd/pii/B9780750650953500027?token=4D1332593D7CA1BAAD37255D01CC0F1E9BF76E727C7F06A589F24C43485FDD8C3A265A4B8AD52E63C696A22022556A38&originRegion=eu-west-1&originCreation=20230413202704> (accessed Apr. 13, 2023).
- [32] D. L. Terrell, ‘Op Amps’, in *Op Amps (Second Edition)*, D. L. Terrell, Ed., Burlington: Newnes, 1996, pp. 173–211. doi: 10.1016/B978-075069702-6/50005-6.
- [33] S. S. Parmar and A. P. Gharge, ‘R-2R ladder circuit design for 32-bit digital-to-analog converter (DAC) with noise analysis and performance parameters’, in *2016 International Conference on Communication and Signal Processing (ICCSP)*, Apr. 2016, pp. 0467–0471. doi: 10.1109/ICCSP.2016.7754180.
- [34] J. R. Baker, *CMOS Circuit Design, Layout, and Simulation*.
- [35] D. Crecraft and D. Gorham, *Electronics*, 2nd ed. London: CRC Press, 2018. doi: 10.1201/9781482268416.
- [36] T. Agarwal, ‘Different Types of Amplifiers with their Working Principle’, *ElProCus - Electronic Projects for Engineering Students*, Jan. 16, 2015. <https://www.elprocus.com/types-of-amplifiers-with-workings/> (accessed Apr. 16, 2023).
- [37] ‘Fundamentals of Electronics, Book 2\_ Amplifiers\_ Analysis and Design.pdf’. Accessed: Apr. 16, 2023. [Online]. Available: [https://nvhrbiblio.nl/biblio/boek/Fundamentals%20of%20Electronics,%20Book%202\\_%20Amplifiers\\_%20Analysis%20and%20Design.pdf](https://nvhrbiblio.nl/biblio/boek/Fundamentals%20of%20Electronics,%20Book%202_%20Amplifiers_%20Analysis%20and%20Design.pdf)
- [38] ‘Operating Point’. [https://www.tutorialspoint.com/amplifiers/operating\\_point.htm](https://www.tutorialspoint.com/amplifiers/operating_point.htm) (accessed Apr. 16, 2023).
- [39] J. M. Fiore, ‘Operational Amplifiers & Linear Integrated Circuits: Theory and Application / 3E’.
- [40] ‘Inverting op amp with non-inverting positive reference voltage circuit’. Accessed: Apr. 16, 2023. [Online]. Available: [https://www.ti.com/lit/an/sboa264a/sboa264a.pdf?ts=1678880084372&ref\\_url=https%253A%252F%252Fwww.startpage.com%252F](https://www.ti.com/lit/an/sboa264a/sboa264a.pdf?ts=1678880084372&ref_url=https%253A%252F%252Fwww.startpage.com%252F)
- [41] ‘Bartels Mikrotechnik, mp6 Electronics Datasheet’. Accessed: Oct. 12, 2022. [Online]. Available: [https://www.bartels-mikrotechnik.de/wp-content/uploads/simple-file-list/EN/Manuals-and-Data-Sheets/mp6\\_electronics\\_Datasheet.pdf](https://www.bartels-mikrotechnik.de/wp-content/uploads/simple-file-list/EN/Manuals-and-Data-Sheets/mp6_electronics_Datasheet.pdf)
- [42] ‘PDU100B-V3-Datasheet-R4.pdf’. Accessed: Dec. 12, 2022. [Online]. Available: [https://www.mmech.com/images/stories/Standard\\_Products/PiezoDrive/PDU100B/PDU100B-V3-Datasheet-R4.pdf](https://www.mmech.com/images/stories/Standard_Products/PiezoDrive/PDU100B/PDU100B-V3-Datasheet-R4.pdf)
- [43] Microchip, ‘Piezoelectric Micropump Driver Reference Design’. 2016. [Online]. Available: <https://ww1.microchip.com/downloads/en/Appnotes/00002104A.pdf>
- [44] D. M. Harris, T. Liu, and J. W. M. Bush, ‘A low-cost, precise piezoelectric droplet-on-demand generator’, *Exp. Fluids*, vol. 56, no. 4, p. 83, Apr. 2015, doi: 10.1007/s00348-015-1950-6.

- [45] Apex Analog, 'Driving Piezoelectric Actuators'.  
<https://www.apexanalog.com/resources/appnotes/an44u.pdf> (accessed May 01, 2023).
- [46] 'PDU100 Micro Piezo Driver | PiezoDrive', Jan. 18, 2016.  
<https://www.piezodrive.com/modules/pdu100-micro-piezo-driver/> (accessed Oct. 12, 2022).
- [47] 'MicroPressure Board Mount Pressure Sensors, MPR Series'.
- [48] '5989-6110.pdf'. Accessed: May 04, 2023. [Online]. Available:  
<https://www.keysight.com/us/en/assets/7018-08449/data-sheets-archived/5989-6110.pdf>
- [49] Bartels Mikrotechnik, 'Instructions for appropriate handling'.  
<https://www.bartels-mikrotechnik.de/wp-content/uploads/simple-file-list/EN/Manuals-and-Data-Sheets/Instructions-for-appropriate-handling.pdf>  
(accessed May 06, 2023).
- [50] N. Gyimah, O. Scheler, T. Rang, and T. Pardy, 'Digital twin for controlled generation of water-in-oil microdroplets with required size', Apr. 2022, pp. 1–7.  
doi: 10.1109/EuroSimE54907.2022.9758876.

## **Appendix 1 – Non-exclusive licence for reproduction and publication of a graduation thesis<sup>1</sup>**

I Rudolf Põldma

1. Grant Tallinn University of Technology free licence (non-exclusive licence) for my thesis “Development of a Prototype Piezoelectric Pump Driver for a Lab-on-Chip Device”, supervised by Rauno Jõemaa
  - 1.1. to be reproduced for the purposes of preservation and electronic publication of the graduation thesis, incl. to be entered in the digital collection of the library of Tallinn University of Technology until expiry of the term of copyright;
  - 1.2. to be published via the web of Tallinn University of Technology, incl. to be entered in the digital collection of the library of Tallinn University of Technology until expiry of the term of copyright.
2. I am aware that the author also retains the rights specified in clause 1 of the non-exclusive licence.
3. I confirm that granting the non-exclusive licence does not infringe other persons' intellectual property rights, the rights arising from the Personal Data Protection Act or rights arising from other legislation.

07.05.2023

---

<sup>1</sup> The non-exclusive licence is not valid during the validity of access restriction indicated in the student's application for restriction on access to the graduation thesis that has been signed by the school's dean, except in case of the university's right to reproduce the thesis for preservation purposes only. If a graduation thesis is based on the joint creative activity of two or more persons and the co-author(s) has/have not granted, by the set deadline, the student defending his/her graduation thesis consent to reproduce and publish the graduation thesis in compliance with clauses 1.1 and 1.2 of the non-exclusive licence, the non-exclusive license shall not be valid for the period.